



This is a repository copy of *High-order cumulants based sparse array design via fractal geometries—part II: robustness and mutual coupling*.

White Rose Research Online URL for this paper:

<https://eprints.whiterose.ac.uk/196799/>

Version: Accepted Version

Article:

Yang, Z. orcid.org/0000-0001-8442-5177, Shen, Q. orcid.org/0000-0002-8295-0442, Liu, W. orcid.org/0000-0003-2968-2888 et al. (2 more authors) (2023) High-order cumulants based sparse array design via fractal geometries—part II: robustness and mutual coupling. IEEE Transactions on Signal Processing, 71. pp. 343-357. ISSN 1053-587X

<https://doi.org/10.1109/tsp.2023.3244667>

© 2023 IEEE. Personal use of this material is permitted. Permission from IEEE must be obtained for all other users, including reprinting/ republishing this material for advertising or promotional purposes, creating new collective works for resale or redistribution to servers or lists, or reuse of any copyrighted components of this work in other works. Reproduced in accordance with the publisher's self-archiving policy.

Reuse

Items deposited in White Rose Research Online are protected by copyright, with all rights reserved unless indicated otherwise. They may be downloaded and/or printed for private study, or other acts as permitted by national copyright laws. The publisher or other rights holders may allow further reproduction and re-use of the full text version. This is indicated by the licence information on the White Rose Research Online record for the item.

Takedown

If you consider content in White Rose Research Online to be in breach of UK law, please notify us by emailing eprints@whiterose.ac.uk including the URL of the record and the reason for the withdrawal request.



eprints@whiterose.ac.uk
<https://eprints.whiterose.ac.uk/>

High-Order Cumulants Based Sparse Array Design via Fractal Geometries—Part II: Robustness and Mutual Coupling

Zixiang Yang, Qing Shen, Wei Liu, *Senior Member, IEEE*, Yonina C. Eldar, *Fellow, IEEE*, Wei Cui

Abstract—Array robustness and mutual coupling are two important factors affecting the direction finding performance of various array structures. These properties are not typically analyzed in DOA estimation based on $2q$ th-order difference co-arrays. In the first part of this work, we proposed fractal arrays for exploiting the $2q$ th-order difference co-array ($2q$ th-O-Fractal). In this second part, we analyze robustness and mutual coupling leakage of the $2q$ th-O-Fractal framework. We introduce a robustness analysis tool, and derive a fragility upper bound on the $2q$ th-O-Fractal as a function of the generator array fragility and the fractal order. Our results show that the robustness of $2q$ th-O-Fractal can be improved by designing a robust generator or increasing the fractal order. The mutual coupling leakage of $2q$ th-O-Fractal is also shown to be upper bounded by that of its generator array. Simulation results demonstrate that the proposed $2q$ th-O-Fractal has superior performance over existing structures exploiting the $2q$ th-order difference co-array, in the presence of random sensor damage and mutual coupling effect.

Index Terms—Sparse array design, difference co-array, high-order cumulants, fractal, direction of arrival estimation.

I. INTRODUCTION

Linear sparse arrays have the ability to resolve far more uncorrelated sources than the number of their physical sensors based on the second-order difference co-array concept [1]–[5]. Notable sparse array structures such as minimum redundancy array (MRA) [6], nested array (NA) [2], and co-prime array (CPA) [1], possess an $\mathcal{O}(N^2)$ -long central uniform linear array (ULA) segment in their second-order difference co-arrays, where N is the number of physical sensors. By exploiting the $2q$ th-order difference co-array (a virtual array arising from vectorizing the $2q$ th-order cumulant matrix of the received data), $\mathcal{O}(N^{2q})$ virtual sensors can be achieved by existing structures known as the $2q$ -level nested array ($2q$ L-NA) [5] and simplified and enhanced $2q$ -level nested array (SE- $2q$ L-NA) [7] with N physical sensors, leading to significantly improved identifiability compared with second-order difference co-array based ones. Note that methods based on high-order cumulants are applicable to non-Gaussian sources only [8]–[13].

With continued development of sparse array design methods, various design criteria have been taken into consideration in designing structures based on the second-order difference co-array, including large consecutive difference co-array, closed-form sensor positions, hole-free difference co-array, robustness and economy, and low mutual coupling [14]–[16]. However, flexible sparse array design incorporating multiple criteria is still a challenging problem for high-order difference co-array exploitation.

The recently proposed flexible fractal array based on the second-order difference co-array (referred to as SO-Fractal) has properties inherited from its simple generator array [14], [15]. Inspired by SO-Fractal, fractal array design based on $2q$ th-order cumulants ($2q$ th-O-Fractal) has been proposed in Part I [17]. To the best of our knowledge, this is the first attempt to consider multiple criteria simultaneously in sparse array design exploiting high-order cumulants. In Part I [17], a closed-form sensor position expression of the $2q$ th-O-Fractal, generated via a joint across-order (across different cumulant order q) and inner-order (within the same cumulant order q) fractal framework, is derived. It is shown that a large consecutive difference co-array ($\mathcal{O}(N^{2q})$ DOFs) can be obtained, with the property of hole-free inheritance discussed for $q = 2$. In this part, two other factors affecting the estimation performance in practical applications, i.e., mutual coupling effect and robustness to sensor failures, are analyzed. Mutual coupling effect reflects the fact that the output of any array sensors is affected in practice by its neighboring sensors [14]. Robustness represents the reliability of difference co-arrays of sparse arrays when sensor loss occurs in practice [18].

Mutual coupling between sensors leads to array model errors [19], [20], resulting in degradation in estimation performance. It is therefore beneficial to include mutual coupling level as a criterion in array design. Sparse arrays with dense subarrays such as NA, have serious deterioration in resolution and estimation performance [21] in the presence of severe mutual coupling. A series of improved NA-like structures such as super nested array (SNA) [20], [22], augmented nested array (ANA) [23], and generalized nested array (GNA) [24] have been proposed, reducing the number of sensor pairs with short spacings while keeping a comparable number of DOFs. Other CPA-like structures recently proposed include coprime array with displaced subarrays (CADiS) [21], thinned coprime array (TCA) [25], and padded coprime arrays (PCA) [26]. These sparse arrays are all designed to exploit the second-order difference co-array. Mutual coupling has not yet been

This work was supported in part by the National Natural Science Foundation of China under Grant 62271052. (Corresponding author: Qing Shen.)

Z. Yang, Q. Shen and W. Cui are with the School of Information and Electronics, Beijing Institute of Technology, Beijing, 100081, China (e-mail: zixiangyang@foxmail.com, qing-shen@outlook.com, cuiwei@bit.edu.cn)

W. Liu is with the Department of Electronic and Electrical Engineering, University of Sheffield, Sheffield, S1 3JD, UK (e-mail: w.liu@sheffield.ac.uk).

Y. C. Eldar is with the Faculty of Mathematics and Computer Science, Weizmann Institute of Science, Rehovot, Israel (e-mail: yonina.eldar@weizmann.ac.il).

introduced to sparse array design based on the $2q$ th-order difference co-array ($q \geq 2$).

Robustness is another important property in practical applications [18], [27]–[31]. Sensor failures could occur randomly and may cause significant performance loss [32]–[35]. Considering the possibility of physical sensor damage, the robustness to sensor failures and stability of co-arrays have been studied recently [18], [27], [28], [36], [37]. In terms of avoiding changes (caused by physical sensor failures) in the difference co-array, the essentialness attribution of each sensor is adopted to evaluate the robustness of the array geometry [18]. Possessing more essential sensors in the array indicates that the virtual array is fragile or less robust when sensor failure occurs. MRA, NA, and Cantor arrays [16] were proven to be maximally economic with all sensors being essential ones, while CPA has relatively superior robustness [27], [38]. Towards the goal of designing more robust array structures, robust MRA (RMRA) [39], composite singer array (CSA) [40], and multiple-fold redundancy array (MFRA) [28], [37] have been presented. Furthermore, a general framework for robustness analysis based on the concept of importance function was proposed in [41], where the importance function characterizes the importance of the subarrays in a structure subject to definable properties related to robustness. However, all these studies focus on sparse arrays exploiting the second-order difference co-arrays. Robustness of sparse arrays based on high-order cumulants has not been analyzed.

In this paper, we focus on the robustness and mutual coupling analysis of the proposed $2q$ th-O-Fractal from [17]. The commonly used tool for robustness analysis (based on the second-order difference co-array) evaluates whether the loss of a physical sensor damages the integrity of the difference co-array [18]. There are N^{2q} virtual sensors (including redundant ones) in the $2q$ th-order difference co-array of an N -sensor physical array. The extremely large number of virtual sensors leads to difficulties in robustness analysis, and the integrity of the entire $2q$ th-order difference co-array could be easily damaged when sensor failure occurs. By extending the quasi-essentialness in [28], we develop a suitable robustness analysis tool for sparse arrays exploiting the $2q$ th-order difference co-array. An importance function describing the change of the consecutive $2q$ th-order difference co-arrays is employed since this consecutive segment can be utilized by various DOA estimation methods, especially subspace-based techniques which are easy to implement. We prove that this importance function belongs to the general robustness analysis framework suggested in [41]. The generalized fragility is defined to evaluate the robustness of arrays subject to the importance function. Then, the inheritance similarity between the robustness of the $2q$ th-O-Fractal and its generator array is confirmed with an upper bound on generalized fragility derived. Finally, the mutual coupling leakage of the proposed $2q$ th-O-Fractal is developed, which is proved to be smaller than that of the generator array.

The contributions of this part are summarized as follows:

1) We extend the idea of quasi-essentialness [28] to the high-order case, and an importance function is presented for robustness evaluation of sparse arrays based on the $2q$ th-order

difference co-array, where the central consecutive co-array segment is taken as a metric to judge whether a sensor/subset is essential or not.

2) The relationship between the robustness of $2q$ th-O-Fractal and the generator array is derived, showing the inheritance similarity between them. After deriving a more precise upper bound on the fragility of SO-Fractal in [14], the fragility upper bound of the $2q$ th-O-Fractal is derived, which is related to the fragility of the generator array and fractal order. We show that, by designing a robust generator array and increasing the fractal order, a more robust $2q$ th-O-Fractal can be obtained.

3) The coupling leakage of $2q$ th-O-Fractal is derived, which is related to the generator, the fractal order r , and the cumulant order q . It is proved that the coupling leakage of the proposed $2q$ th-O-Fractal is upper bounded by that of its generator array. By designing a generator array with low coupling leakage, the mutual coupling effect on DOA estimation performance of the $2q$ th-O-Fractal can be reduced.

4) To the best of our knowledge, this is the first study to consider robustness and mutual coupling in array design exploiting high-order cumulants. The proposed $2q$ th-O-Fractal can be generated by considering the criterion of either high robustness or low mutual coupling. More importantly, $2q$ th-O-Fractal can be flexibly designed with both low fragility and small mutual coupling leakage, leading to better performance than existing structures in the presence of random sensor damage and mutual coupling effect.

The paper is organized as follows. Section II reviews preliminaries of the $2q$ th-order difference co-array, structure of the proposed $2q$ th-O-Fractal, and design criteria. The robustness analysis tool for sparse arrays exploiting the $2q$ th-order difference co-array is presented in Section III. Array robustness of the proposed structure is analyzed in Section IV, while mutual coupling leakage is studied in Section V. Examples and simulation results are provided in Section VI, and conclusions are drawn in Section VII.

II. PRELIMINARIES

A. The $2q$ th-Order Difference Co-Array

Here we focus on narrowband far-field source signals that are non-Gaussian and independent of each other [17]. By vectorizing the $2q$ th-order cumulant matrix of the received data, a virtual array model with manifold corresponding to the $2q$ th-order difference co-array is obtained. The set of the $2q$ th-order difference co-array [5], [7], [42] of an N -sensor array \mathbb{A} is defined as

$$\mathbb{D}_{2q} = \left\{ \sum_{k=1}^q \mu_k - \sum_{l=q+1}^{2q} \mu_l \mid \mu_k, \mu_l \in \mathbb{A} \right\}. \quad (1)$$

More background information can be found in the companion Part I [17].

Specifically, $\mathcal{O}(N^{2q})$ unique virtual sensors can be provided by \mathbb{D}_{2q} for array structures such as $2q$ L-NA [5], SE- $2q$ L-NA [7], and the proposed $2q$ th-O-Fractal in Part I with specifically selected generator array [17]. This implies that the number of unique co-array lags cannot exceed $\mathcal{O}(N^2)$ in case of the second-order difference co-array (i.e., $q = 1$). In the

commonly used subspace-based methods such as SS-MUSIC [2], [5], [43], only the central ULA segment of the co-array can be utilized for estimation [5]. Therefore, the central ULA segment is taken as a metric in analyzing the sensor essentialness in Section III.

B. SO-Fractal and 2qth-O-Fractal

Inspired by fractal array exploiting the second-order difference co-array (SO-Fractal) [14], [15], a new structure, i.e., the fractal array based on the 2qth-order difference co-array (2qth-O-Fractal) was proposed in the companion Part I [17]. Due to the superiority in property inheritance from the generator array, the array construction problem is translated into designing an appropriate simple generator array with given requirements. In this subsection, the structures of SO-Fractal and 2qth-O-Fractal are reviewed briefly.

The SO-Fractal with a generator array \mathbb{G} is expressed as [14], [15]

$$\begin{aligned} \mathbb{F}_0 &\triangleq \{0\}, \\ \mathbb{F}_{r+1} &\triangleq \bigcup_{n \in \mathbb{G}} (\mathbb{F}_r + nM^r), r \in \mathbb{N}^+, \end{aligned} \quad (2)$$

where $M \triangleq |\mathbb{U}|$ with $|\cdot|$ returning the cardinality of the input set, \mathbb{U} is the longest central ULA segment in the second-order difference co-array of \mathbb{G} , and r is the fractal order belonging to the set of positive integers \mathbb{N}^+ . As proved in [14], the second-order difference co-array of \mathbb{F}_r (denoted by \mathbb{D}_2) contain consecutive co-array lags in $\mathbb{U}_{2(\mathbb{F}_r)} = [-\frac{M^r-1}{2}, \frac{M^r-1}{2}]$.

The 2qth-O-Fractal is proposed in the companion paper (Part I [17]), aiming at forming a flexible sparse array structure with inheritance similarity to the generator \mathbb{G} . The 2qth-O-Fractal is defined as follows [17].

Definition 1: The 2qth-O-Fractal $\mathbb{E}_r^{2q} = \bigcup_{h=1}^q \mathbb{E}_r(h)$ consists of q subarrays, i.e., $\mathbb{E}_r(1), \mathbb{E}_r(2), \dots, \mathbb{E}_r(q)$, where

$$\mathbb{E}_r(1) \triangleq \bigcup_{n \in \mathbb{F}_r} (n \cdot T_1 + m_1) = \mathbb{F}_r, \quad (3)$$

$$\mathbb{E}_r(2) \triangleq \bigcup_{n \in \mathbb{E}_r(1)} (n \cdot T_2 + m_2), \quad (4)$$

⋮

$$\mathbb{E}_r(q) \triangleq \bigcup_{n \in \mathbb{E}_r(1)} (n \cdot T_q + m_q). \quad (5)$$

The original SO-Fractal is denoted by \mathbb{F}_r . The expanding factor T_q and the offset term m_q are defined by recursive expressions, given by

$$\begin{aligned} T_0 &= 0, T_1 = 1, \\ T_q &= M^r \cdot T_{q-1} + (M^r - 1) \cdot T_{q-2}, q \geq 2, \end{aligned} \quad (6)$$

$$\begin{aligned} m_0 &= 0, m_1 = 0, \\ m_q &= -f_{r(j)} \cdot T_q + f_{r(i)} \cdot T_{q-1} + m_{q-1}, q \geq 2, \end{aligned} \quad (7)$$

where $(f_{r(i)}, f_{r(j)}) \in \mathbb{E}_r^2 = \mathbb{F}_r^2$ is a pair of sensors satisfying $f_{r(i)} - f_{r(j)} = \max(\mathbb{U}_{2(\mathbb{F}_r)}) = \frac{M^r-1}{2}$ (see Lemma 1 in Part I [17]). The expanding factor T_q is defined as the number of guaranteed central ULA sensors in the $2(q-1)$ th-order

difference co-array of the $2(q-1)$ th-O-Fractal $\mathbb{E}_r^{2(q-1)} = \bigcup_{h=1}^{q-1} \mathbb{E}_r(h)$, which is also the unit inter-element spacing of the q -th subarray. The offset m_q in (7) is constructed based on the idea that a common physical sensor is shared by the subarrays with adjacent indices, i.e., $\mathbb{E}_r(q-1)$ and $\mathbb{E}_r(q)$. The above across-order fractal design ensures structural similarity across cumulant order q (also considered as an across-order fractal factor).

Within the p th-level subarray ($1 \leq p \leq q$), the variation of sensor positions with the fractal order r (inner-order fractal factor within the same cumulant order) can be expressed as

$$\begin{aligned} \mathbb{E}_{0(p)} &= \{m_p\}, \\ \mathbb{E}_{r(p)} &= \bigcup_{n \in \mathbb{E}_r(1)} (n \cdot T_p + m_p) \\ &= \bigcup_{u \in \mathbb{G}} (\mathbb{E}_{r-1(1)} \cdot T_p + u \cdot T_p M^{r-1} + m_p), r \in \mathbb{N}^+, \end{aligned} \quad (8)$$

where $M \triangleq |\mathbb{U}|$ is the length of the central ULA segment in the second-order difference co-array of the generator \mathbb{G} . An example is given in Fig. 1 to demonstrate the structure of 2qth-O-Fractal.

C. Sparse Array Design–Robustness and Mutual Coupling

In the companion paper (Part I [17]), five criteria of interest are listed for sparse array design, i.e., 1: *Large consecutive difference co-array*, 2: *Closed-form sensor positions*, 3: *Hole-free difference co-array*, 4: *Robustness and economy*, and 5: *Low mutual coupling*. For 2qth-O-Fractal, the first three criteria have been analyzed and discussed, verifying the superiority of the proposed framework in incorporating these properties via optimizing the generator array. In this part, we focus on the relevant properties of *Criterion 4: Robustness and economy* and *Criterion 5: Low mutual coupling* of the proposed framework, and their definitions are given below.

Criterion 4 (Robustness and economy): The difference co-array structure of a sparse array is susceptible to sensor failures, which are likely to occur in practical applications [18]. When reliability is important, the sparse array structure should be highly robust to sensor failures, implying that the loss of elements has as little effect as possible on the generated co-array [27]. When the physical sensors are expensive, maximally economic arrays are more attractive, ensuring that each sensor is essential and indispensable with respect to the co-array of interest [16], [27].

Criterion 5 (Low mutual coupling): In practice, any sensor output is affected by its neighboring sensors. This electromagnetic interaction phenomenon is called mutual coupling [14]. Mutual coupling has an adverse effect on DOA estimation performance [19]–[21], and thus it is desirable to design sparse arrays with low mutual coupling.

Previous works on robustness mainly focused on the second-order difference co-array of a physical array (denoted by \mathbb{D}_2). If the removal of a sensor results in a change in \mathbb{D}_2 , this sensor is considered as an essential one; otherwise, it is inessential [18]. An example is given to illustrate the concept of essential sensors in Fig. 2. However, the robustness analysis for sparse

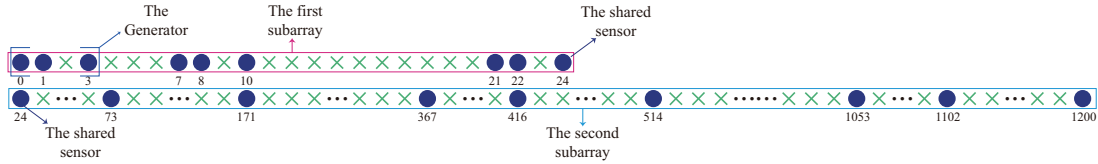


Fig. 1. An example of $2q$ th-O-Fractal with generator array $\mathbb{G} = \{0, 1, 3\}$, fractal order $r = 2$, and cumulant order $q = 2$.

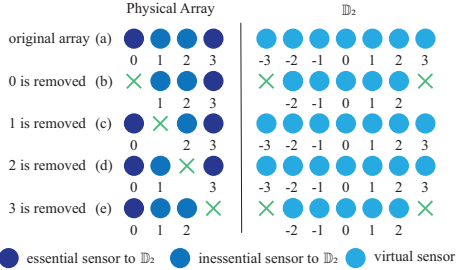


Fig. 2. An illustration of the essentialness with respect to the second-order difference co-array \mathbb{D}_2 . The original array in (a) is a ULA with 4 physical sensors. The removal of essential sensors causes a reduction in \mathbb{D}_2 (as shown in (b), (e)), while the removal of inessential sensors does not (as shown in (c), (d)).

arrays based on high-order cumulants has not been discussed, where the substantially increased number of virtual sensors in the $2q$ th-order difference co-array results in extremely high complexity in robustness analysis.

From the perspective of array design, the mutual coupling effect of different array structures can be evaluated by coupling leakage, and can be reduced by increasing the distance between adjacent sensors as much as possible. The definition of mutual coupling matrix and coupling leakage will be given in Section V.

III. ROBUSTNESS ANALYSIS TOOL

In order to analyze the array robustness from the high-order difference co-array perspective effectively, in this section we introduce necessary evaluation tools.

The traditional definition of essential sensor is to judge whether a sensor failure destroys the integrity of the second-order difference co-array [18], [27], [38], [44] or not. It can be extended to the high-order case by checking whether the integrity of the $2q$ th-order difference co-array is damaged by the loss of a physical sensor. Due to the massively increased number of virtual sensors (at most N^{2q} including redundant ones) in the $2q$ th-order difference co-array, it is difficult to evaluate the essentialness of physical sensors via theoretical analysis and numerical verification.

The concept of quasi-essential sensors presented in [28] focuses on the integrity of the consecutive second-order difference co-array. In [41], a general analysis framework for robustness was proposed, which allows one to customize the importance function to form a generalized fragility metric suitable for robustness analysis of sparse structures.

Commonly adopted subspace-based methods can only exploit the information provided by the consecutive difference co-array segment. Since the consecutive segment can be easily utilized by various DOA estimation techniques, focusing on

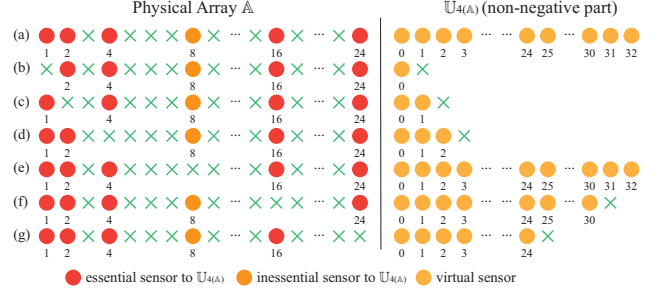


Fig. 3. An illustration of the essentialness with respect to the central ULA segments $\mathbb{U}_{2q(\mathbb{A})}$. The original array in (a) is $2q$ L-NA ($q = 2$) with 6 physical sensors. The removal of essential sensors causes reduction in the central ULA segment of the fourth-order difference co-array (as shown in (b)-(d) and (f)-(g)), while the removal of inessential sensors does not (as shown in (e)).

the consecutive segment in the $2q$ th-order difference co-array instead of the entire co-array is more important in practice. Inspired by these works, we present the definition of essentialness with respect to the consecutive $2q$ th-order difference co-array segment as follows.

Definition 2: Consider the central ULA segment $\mathbb{U}_{2q(\mathbb{A})}$ guaranteed in the $2q$ th-order difference co-array \mathbb{D}_{2q} of array \mathbb{A} . For a subset $\mathbb{A}_s \subseteq \mathbb{A}$, the $2q$ th-order difference co-array after removing \mathbb{A}_s from available sensors' collection ($\mathbb{A} \setminus \mathbb{A}_s$) is denoted by $\overline{\mathbb{D}}_{2q(\mathbb{A}_s)}$. The sensor set \mathbb{A}_s is $|\mathbb{A}_s|$ -essential with respect to the central ULA segment if $\mathbb{U}_{2q(\mathbb{A})} \not\subseteq \overline{\mathbb{D}}_{2q(\mathbb{A}_s)}$, while $|\mathbb{A}_s|$ -inessential if $\mathbb{U}_{2q(\mathbb{A})} \subseteq \overline{\mathbb{D}}_{2q(\mathbb{A}_s)}$.

In particular, if we set $|\mathbb{A}_s| = 1$, then the above definition becomes the evaluation of essentialness for each sensor with respect to $\mathbb{U}_{2q(\mathbb{A})}$. Furthermore, if we set $q = 1$, $|\mathbb{A}_s| = 1$, and assume \mathbb{D}_{2q} is hole-free (i.e., $\mathbb{D}_{2q} = \mathbb{U}_{2q(\mathbb{A})}$), then **Definition 2** is equivalent to the conventional definition based on the second-order difference co-array [44]. An example to explain the concept of essentialness with respect to $\mathbb{U}_{2q(\mathbb{A})}$ is shown in Fig. 3.

We next define an importance function \mathcal{I}_{ce} and prove that \mathcal{I}_{ce} meets the required properties under the robustness analysis framework in **Corollary 1**, and thus \mathcal{I}_{ce} is appropriate to evaluate array robustness.

Definition 3: Consider an array \mathbb{A} with the central ULA segment $\mathbb{U}_{2q(\mathbb{A})}$ in its $2q$ th-order difference co-array \mathbb{D}_{2q} . The importance function associated with $\mathbb{U}_{2q(\mathbb{A})}$ is defined as

$$\mathcal{I}_{ce}(\mathbb{A}_s) = \begin{cases} 1, & \text{if } \mathbb{A}_s \text{ is } |\mathbb{A}_s|\text{-essential for } \mathbb{U}_{2q(\mathbb{A})}, \\ 0, & \text{otherwise.} \end{cases} \quad (9)$$

In the following **Corollary 1**, we show that \mathcal{I}_{ce} satisfies the required properties of the general framework for robustness analysis suggested in [41], proving that it is a suitable tool to quantify array robustness.

Corollary 1: The importance function \mathcal{I}_{ce} satisfies the following required properties [41]:

- $0 \leq \mathcal{I}_{ce}(\mathbb{A}_s) \leq 1$ for all $\mathbb{A}_s \subseteq \mathbb{A}$.
- $\mathcal{I}_{ce}(\emptyset) = 0$ and $\mathcal{I}_{ce}(\mathbb{A}) = 1$.
- \mathcal{I}_{ce} is monotone which implies $\mathcal{I}_{ce}(\mathbb{B}_1) \leq \mathcal{I}_{ce}(\mathbb{B}_2)$ for $\mathbb{B}_1 \subseteq \mathbb{B}_2 \subseteq \mathbb{A}$.

Proof: First, according to *Definition 3*, \mathcal{I}_{ce} is either 0 or 1, so $0 \leq \mathcal{I}_{ce}(\mathbb{A}_s) \leq 1$ is obviously true.

Second, if $\mathbb{A}_s = \emptyset$, we have $\mathbb{U}_{2q(\mathbb{A})} \subseteq \overline{\mathbb{D}}_{2q(\emptyset)} = \mathbb{D}_{2q}$ and thus $\mathcal{I}_{ce}(\emptyset) = 0$. On the other hand, if $\mathbb{A}_s = \mathbb{A}$, we have $\mathbb{U}_{2q(\mathbb{A})} \not\subseteq \overline{\mathbb{D}}_{2q(\mathbb{A})} = \emptyset$ and $\mathcal{I}_{ce}(\mathbb{A}) = 1$.

Third, if $\mathbb{B}_1 \subseteq \mathbb{B}_2 \subseteq \mathbb{A}$, then, the subset $\mathbb{A} \setminus \mathbb{B}_2 \subseteq \mathbb{A} \setminus \mathbb{B}_1$, leading to $\overline{\mathbb{D}}_{2q(\mathbb{B}_2)} \subseteq \overline{\mathbb{D}}_{2q(\mathbb{B}_1)}$. Therefore, $\overline{\mathbb{D}}_{2q(\mathbb{B}_2)}$ is more likely to no longer contain $\mathbb{U}_{2q(\mathbb{A})}$, which implies $\mathcal{I}_{ce}(\mathbb{B}_1) \leq \mathcal{I}_{ce}(\mathbb{B}_2)$. ■

Based on the importance function \mathcal{I}_{ce} , the generalized 1-fragility is defined as follows.

Definition 4: Consider an array \mathbb{A} with the central ULA segment $\mathbb{U}_{2q(\mathbb{A})}$ in its $2q$ th-order difference co-array. The 1-fragility $F_1(\mathbb{A}, \mathcal{I}_{ce})$ related to \mathbb{A} and importance function \mathcal{I}_{ce} is defined as

$$F_1(\mathbb{A}, \mathcal{I}_{ce}) \triangleq \sum_{\mathbb{A}_s \subseteq \mathbb{A}, |\mathbb{A}_s|=1} \frac{\mathcal{I}_{ce}(\mathbb{A}_s)}{\binom{|\mathbb{A}|}{1}} = \frac{N_{ce}}{|\mathbb{A}|}, \quad (10)$$

where $\binom{|\mathbb{A}|}{1}$ is the binomial coefficient, and N_{ce} denotes the number of essential sensors with respect to $\mathbb{U}_{2q(\mathbb{A})}$.

The definition of the maximally economic array in [16], [27] can be extended to the scenario based on the essentialness with respect to virtual ULA in the $2q$ th-order difference co-array $\mathbb{U}_{2q(\mathbb{A})}$ rather than the essentialness with respect to the entire difference co-array.

Definition 5: Consider an array \mathbb{A} with the central ULA segment $\mathbb{U}_{2q(\mathbb{A})}$ in its $2q$ th-order difference co-array. The array \mathbb{A} is maximally economic with respect to $\mathbb{U}_{2q(\mathbb{A})}$ if all sensors in \mathbb{A} are essential for $\mathbb{U}_{2q(\mathbb{A})}$. In other words, \mathbb{A} is maximally economic with respect to $\mathbb{U}_{2q(\mathbb{A})}$ if $F_1(\mathbb{A}, \mathcal{I}_{ce}) = \frac{|\mathbb{A}|}{|\mathbb{A}|} = 1$.

Based on the essentialness in *Definition 2*, the importance function is introduced in *Definition 3*, which leads to the quantitative robustness metric of 1-fragility in *Definition 4*. *Definition 5* is an example, explaining the relationship between the maximally economic array and 1-fragility. The quantitative metric 1-fragility will be used to analyze the robustness of $2q$ th-O-Fractal in *Lemma 2* and *Proposition 2* in the next section.

IV. ROBUSTNESS ANALYSIS

In this section, robustness of the original SO-Fractal is first analyzed in detail. Then, the tool presented in Section III is utilized to analyze the robustness of the proposed $2q$ th-O-Fractal, establishing the robustness relationship between the $2q$ th-O-Fractal and its generator array.

A. Robustness Analysis of the SO-Fractal

By analyzing the robustness of the SO-Fractal, we have the following *Lemma 1*.

Lemma 1: For the original SO-Fractal with fractal order $r+1$ defined in (2), i.e.,

$$\begin{aligned} \mathbb{F}_{r+1} &= \bigcup_{n \in \mathbb{G}} (\mathbb{F}_r + nM^r) \\ &= \{l + nM^r \mid l \in \mathbb{F}_r, n \in \mathbb{G}\}, \end{aligned} \quad (11)$$

the following properties are valid:

- If $n_1 \in \mathbb{G}$ is inessential with respect to \mathbb{D}_G , then the element $l_1 + n_1M^r \in \mathbb{F}_{r+1}$ is inessential with respect to \mathbb{D}_{r+1} for all $l_1 \in \mathbb{F}_r$.
- If $l_2 \in \mathbb{F}_r$ is inessential with respect to \mathbb{D}_r , then the element $l_2 + n_2M^r \in \mathbb{F}_{r+1}$ is inessential with respect to \mathbb{D}_{r+1} for all $n_2 \in \mathbb{G}$.

Here \mathbb{D}_G and \mathbb{D}_{r+1} are the second-order difference co-array of the generator array \mathbb{G} and \mathbb{F}_{r+1} , respectively.

Proof: The second-order difference co-array of \mathbb{F}_{r+1} can be represented by $\mathbb{D}_{r+1} = \mathbb{D}_r + M^r\mathbb{D}_G$. Assume that $n_1 \in \mathbb{G}$ is inessential with respect to \mathbb{D}_G , which implies that the difference co-array $\overline{\mathbb{D}}_G$ of $\mathbb{G} \setminus \{n_1\}$ is the same as \mathbb{D}_G . Therefore, the difference co-array $\overline{\mathbb{D}}_{r+1}$ of $\overline{\mathbb{F}}_{r+1} = \{l + nM^r \mid l \in \mathbb{F}_r, n \in \mathbb{G} \setminus \{n_1\}\}$ is identical to \mathbb{D}_{r+1} , since $\overline{\mathbb{D}}_{r+1} = \mathbb{D}_r + M^r\overline{\mathbb{D}}_G = \mathbb{D}_r + M^r\mathbb{D}_G = \mathbb{D}_{r+1}$. Obviously, the element $l_1 + n_1M^r$ belongs to the set $\mathbb{F}_{r+1} \setminus \overline{\mathbb{F}}_{r+1}$, and thus the element $l_1 + n_1M^r$ is inessential with respect to \mathbb{D}_{r+1} .

Similarly, if $l_2 \in \mathbb{F}_r$ is inessential with respect to \mathbb{D}_r , then the difference co-array $\overline{\mathbb{D}}_r$ of $\mathbb{F}_r \setminus \{l_2\}$ is the same as \mathbb{D}_r . Therefore, the difference co-array $\overline{\mathbb{D}}_{r+1}$ of $\overline{\mathbb{F}}_{r+1} = \{l + nM^r \mid l \in \mathbb{F}_r \setminus \{l_2\}, n \in \mathbb{G}\}$ is identical to \mathbb{D}_{r+1} since $\overline{\mathbb{D}}_{r+1} = \overline{\mathbb{D}}_r + M^r\mathbb{D}_G = \mathbb{D}_r + M^r\mathbb{D}_G = \mathbb{D}_{r+1}$. It is noted that the element $l_2 + n_2M^r$ belongs to the set $\mathbb{F}_{r+1} \setminus \overline{\mathbb{F}}_{r+1}$, and thus the element $l_2 + n_2M^r$ is inessential with respect to \mathbb{D}_{r+1} . ■

Based on inheritance property of inessential sensors proved in *Lemma 1*, the fragility relationship between the SO-Fractal and its generator array is given in the following proposition.

Proposition 1: Consider the SO-Fractal \mathbb{F}_r generated from generator \mathbb{G} with hole-free second-order difference co-array. The fragility of \mathbb{F}_r and \mathbb{G} satisfies

$$F_r \leq F_G^r, \quad r \in \mathbb{N}^+, \quad (12)$$

with

$$F_r = \frac{N_{er}}{N_G^r}, \quad F_G = \frac{N_{eG}}{N_G}, \quad (13)$$

where F_r and F_G denote the fragility of \mathbb{F}_r and \mathbb{G} , respectively, and N_{er} and N_{eG} represent the number of essential sensors in \mathbb{F}_r and \mathbb{G} , respectively. N_G is the number of sensors in \mathbb{G} .

Proof: According to (13), (12) is equivalent to

$$N_{er} \leq N_{eG}^r, \quad r \in \mathbb{N}^+. \quad (14)$$

(14) can be proved by mathematical induction.

For $r = 1$, $N_{e1} = N_{eG}^1$ since $\mathbb{F}_1 = \mathbb{G}$. For $r = k$, assume $N_{ek} \leq N_{eG}^k$. Then for $r = k + 1$, we focus on the inessential sensors with respect to \mathbb{D}_{r+1} . The sets of inessential sensors in \mathbb{G} with respect to \mathbb{D}_G and inessential sensors in \mathbb{F}_k with

respect to \mathbb{D}_k are represented by \mathbb{G}_{in} and $\mathbb{F}_{k,\text{in}}$. According to *Lemma 1*, the sensors in the following sets,

$$\begin{aligned}\mathbb{I}_1 &= \{l + nM^r \mid l \in \mathbb{F}_k, n \in \mathbb{G}_{\text{in}}\}, \\ \mathbb{I}_2 &= \{l + nM^r \mid l \in \mathbb{F}_{k,\text{in}}, n \in \mathbb{G}\},\end{aligned}\quad (15)$$

are all inessential sensors in \mathbb{F}_{k+1} with respect to \mathbb{D}_{k+1} . Note that \mathbb{I}_1 and \mathbb{I}_2 have an intersection

$$\mathbb{I}_3 = \mathbb{I}_1 \cap \mathbb{I}_2 = \{l + nM^r \mid l \in \mathbb{F}_{k,\text{in}}, n \in \mathbb{G}_{\text{in}}\}.\quad (16)$$

Therefore, the number of inessential sensors in \mathbb{F}_{k+1} with respect to \mathbb{D}_{k+1} (denoted by N_{k+1}) satisfies

$$\begin{aligned}N_{k+1} &\geq |\mathbb{I}_1 \cup \mathbb{I}_2| = |\mathbb{I}_1| + |\mathbb{I}_2| - |\mathbb{I}_3| \\ &= |\mathbb{F}_k| \cdot |\mathbb{G}_{\text{in}}| + |\mathbb{F}_{k,\text{in}}| \cdot |\mathbb{G}| - |\mathbb{F}_{k,\text{in}}| \cdot |\mathbb{G}_{\text{in}}| \\ &= N_G^k \cdot (N_G - N_{eG}) + (N_G^k - N_{ek}) \cdot N_{eG}.\end{aligned}\quad (17)$$

As a result, the number of essential sensors in \mathbb{F}_{k+1} with respect to \mathbb{D}_{k+1} is

$$\begin{aligned}N_{e(k+1)} &= N_G^{k+1} - N_{k+1} \\ &\leq N_G^{k+1} - N_G^k \cdot (N_G - N_{eG}) - (N_G^k - N_{ek}) \cdot N_{eG} \\ &= N_{ek} \cdot N_{eG}.\end{aligned}\quad (18)$$

Finally, $N_{e(k+1)} \leq N_{ek} \cdot N_{eG} \leq N_{eG}^{k+1}$ is obtained, which completes the proof. \blacksquare

Eq. (12) is an extension of Theorem 6 in [14], where $F_r \leq F_G$ is proven. With assistance of the inheritance property of inessential sensors given in *Lemma 1*, a more accurate upper bound of fragility for each fractal order r , i.e., $F_r \leq F_G^r$ ($r \in \mathbb{N}^+$ and $0 \leq F_G \leq 1$), is derived in *Proposition 1*, which implies that a more robust SO-Fractal structure can be obtained if a higher fractal order r is utilized.

The conclusion of *Proposition 1* motivates us to explore whether there is a similar conclusion for the robustness of 2qth-O-Fractal. To answer this, robustness of the proposed 2qth-O-Fractal is analyzed in the following subsection.

B. Robustness Analysis of the Proposed 2qth-O-Fractal

To simplify the robustness analysis of 2qth-O-Fractal, the core composition (see *Definition 6*) is introduced.

Recall the definition of the 2qth-order difference co-array of a sparse array \mathbb{A} , which is $\mathbb{D}_{2q} = \{\sum_{k=1}^q \mu_k - \sum_{l=q+1}^{2q} \mu_l \mid \mu_k, \mu_l \in \mathbb{A}\}$. Denote $\mathbb{A}_1, \mathbb{A}_2, \dots$, and \mathbb{A}_{2q} as subsets of \mathbb{A} . The set obtained by restricting $\mu_p \in \mathbb{A}_p$ ($p = 1, 2, \dots, 2q$), i.e.,

$$\Phi_{2q} = \left\{ \sum_{k=1}^q \mu_k - \sum_{l=q+1}^{2q} \mu_l \mid \mu_1 \in \mathbb{A}_1, \dots, \mu_{2q} \in \mathbb{A}_{2q} \right\},$$

is called a component of \mathbb{D}_{2q} . Since there are many options for each \mathbb{A}_p ($1 \leq p \leq 2q$), numerous components exist.

Definition 6: The core composition is a component of \mathbb{D}_{2q} , which can completely cover the central ULA segment \mathbb{U}_{2q} guaranteed in \mathbb{D}_{2q} , i.e.,

$$\mathbb{D}_{2q} \supseteq \Phi_{2q} \supseteq \mathbb{U}_{2q}.\quad (19)$$

With the assistance of the transitivity in (19), part of inessential sensors in each subarray of 2qth-O-Fractal can be identified, as shown in *Lemma 2*.

Lemma 2: Consider the 2qth-O-Fractal ($q \geq 1$) $\mathbb{E}_r^{2q} = \bigcup_{l=1}^q \mathbb{E}_{r(l)}$ generated from the generator array \mathbb{G} with hole-free second-order difference co-array. Here $\mathbb{U}_{2q(\mathbb{E}_r)}$ denotes the central ULA segment guaranteed in \mathbb{D}_{2q} (the 2qth-order difference co-array of 2qth-O-Fractal). The sensors in $\mathbb{I}_r^{2q} = \bigcup_{l=1}^q \mathbb{I}_{r(l)}$ are all inessential with respect to $\mathbb{U}_{2q(\mathbb{E}_r)}$, where

$$\mathbb{I}_{r(l)} \triangleq \bigcup_{n \in \mathbb{I}_{r(1)}} (n \cdot T_l + m_l)\quad (20)$$

and $\mathbb{I}_{r(1)}$ is the set of inessential sensors in SO-Fractal for $q = 1$. T_l and m_l denote the expansion factor and offset term of the l -th level subarray in 2qth-O-Fractal, determined by (6) and (7), respectively.

Proof: See Appendix A. \blacksquare

Next, we derive the upper bound on fragility of 2qth-O-Fractal. The relationship between the robustness of 2qth-O-Fractal and its generator array in terms of the generalized 1-fragility is demonstrated, reflecting the robustness inheritance property of the 2qth-O-Fractal.

Proposition 2: Consider the 2qth-O-Fractal ($q \geq 1$) $\mathbb{E}_r^{2q} = \bigcup_{l=1}^q \mathbb{E}_{r(l)}$ generated from \mathbb{G} with hole-free second-order difference co-array. Then, the 1-fragility $F_1(\mathbb{E}_r^{2q}, \mathcal{J}_{ce})$ related to the sparse array \mathbb{E}_r^{2q} and importance function \mathcal{J}_{ce} satisfies

$$F_1(\mathbb{E}_r^{2q}, \mathcal{J}_{ce}) \leq \frac{qF_G^r N_G^r - q + 1}{qN_G^r - q + 1} \leq F_G^r, r \in \mathbb{N}^+.\quad (21)$$

Note that q and r are cumulant order and fractal order, respectively. The parameters N_G and F_G represent the number of sensors in \mathbb{G} and the fragility of \mathbb{G} .

Proof: According to the definition of 1-fragility $F_1(\mathbb{E}_r^{2q}, \mathcal{J}_{ce})$ (see *Definition 4*), the essential sensors with respect to $\mathbb{U}_{2q(\mathbb{E}_r)}$ are analyzed. Here $\mathbb{U}_{2q(\mathbb{E}_r)}$ denotes the central ULA segment guaranteed in \mathbb{D}_{2q} (the 2qth-order difference co-array of 2qth-O-Fractal).

The number of physical sensors in \mathbb{E}_r^{2q} is $N(q) = qN_G^r - q + 1$, where N_G is the number of physical sensors in \mathbb{G} .

As proved in *Lemma 2*, the sensors in \mathbb{I}_r^{2q} are all inessential, and the number of inessential sensors satisfies

$$N_{\text{ine}}(q) \geq |\mathbb{I}_r^{2q}| = q \cdot |\mathbb{I}_{r(1)}|.\quad (22)$$

According to the proof of *Proposition 1*, the number of inessential sensors in SO-Fractal holds

$$|\mathbb{I}_{r(1)}| = N_G^r - N_{er} \geq N_G^r - N_{eG}^r.\quad (23)$$

Therefore, the number of essential sensors in 2qth-O-Fractal satisfies

$$\begin{aligned}N_{\text{ce}}(q) &= N(q) - N_{\text{ine}}(q) \\ &\leq qN_G^r - q + 1 - q(N_G^r - N_{eG}^r) \\ &= qN_{eG}^r - q + 1.\end{aligned}\quad (24)$$

TABLE I
EXAMPLES OF THE FRAGILITY

Structures \mathbb{E}_r^{2q}	Number of Sensors	Generator Array	Fragility $F_1(\mathbb{E}_r^{2q}, \mathcal{I}_{ce})$	Upper Bound F_G^r
\mathbb{E}_1^2	10	\mathbb{G}_1	0.3	0.3
\mathbb{E}_2^2	100	\mathbb{G}_1	0.09	0.09
\mathbb{E}_3^2	1000	\mathbb{G}_1	0.027	0.027
\mathbb{E}_1^3	11	\mathbb{S}_1	0.27	0.27
\mathbb{E}_2^3	121	\mathbb{S}_1	0.03	0.0729
\mathbb{E}_3^3	1331	\mathbb{S}_1	0.006	0.0197
\mathbb{E}_1^2	4	\mathbb{L}	0.5	0.5
\mathbb{E}_2^2	16	\mathbb{L}	0.25	0.25
\mathbb{E}_3^2	64	\mathbb{L}	0.125	0.125
\mathbb{E}_1^4	7	\mathbb{L}	0.1429	0.5
\mathbb{E}_2^4	31	\mathbb{L}	0.0323	0.25
\mathbb{E}_3^4	127	\mathbb{L}	0.0079	0.125

Finally, according to *Definition 4*,

$$\begin{aligned}
 F_1(\mathbb{E}_r^{2q}, \mathcal{I}_{ce}) &= \frac{N_{ce}(q)}{N(q)} \leq \frac{qN_{eG}^r - q + 1}{qN_G^r - q + 1} \\
 &= \frac{qF_G^r N_G^r - q + 1}{qN_G^r - q + 1} \leq \frac{qF_G^r N_G^r - qF_G^r + F_G^r}{qN_G^r - q + 1} \\
 &= F_G^r,
 \end{aligned} \tag{25}$$

which completes the proof. \blacksquare

C. Comparisons of Robustness

Proposition 1 and *Proposition 2* are demonstrated through robustness comparisons of different array structures.

In [14], two generator arrays

$$\mathbb{G}_1 = \{0, 1, 3, 5, 11, 13, 17, 18, 19, 20\}, \tag{26}$$

$$\mathbb{S}_1 = \{0, 1, 2, 4, 7, 10, 13, 16, 18, 19, 20\}, \tag{27}$$

with good properties are employed, and the fragilities of the SO-Fractal arrays generated by them with fractal order $r = 2$ and $r = 3$ are analyzed. Using the same structures, their respective fragility upper bounds are calculated, as shown in Table I. From the top half of the table, it is clear that the relationship $F_r \leq F_G^r$ is satisfied.

Next, the proposed fractal arrays based on different cumulants order q are considered in comparison, and $\mathbb{L} = \{0, 1, 2, 3\}$ is chosen as the generator with two inessential sensors at 1 and 2. As shown in the lower part of Table I, the fragility relationship $F_1(\mathbb{E}_r^{2q}, \mathcal{I}_{ce}) \leq F_G^r$ holds true consistently.

Proposition 1 and *Proposition 2* present a direct relationship between the robustness of $2q$ th-O-Fractal and the generator \mathbb{G} , reflecting the transitivity of the array robustness provided by the fractal method. The fractal method leads to structures exploiting high-order difference co-array with an upper bounded fragility. This is beneficial to array design with high robustness to sensor failures since heavy searches or case-by-case discussions on array potential configurations can be avoided. *Proposition 2* provides a simple way to construct a robust large array by designing a robust generator array \mathbb{G} and increasing the fractal order r . In addition, the difference co-array redundancies increase with the fractal order, resulting

in reduced number of uDOFs with respect to the number of physical sensors [14].

V. MUTUAL COUPLING IN $2q$ TH-O-FRACTAL

Considering *Criterion 5 (Low mutual coupling)* in sparse array design, in the presence of mutual coupling, the original array signal model is usually modified to

$$\mathbf{x}[i] = \mathbf{C}_m \mathbf{A}(\theta) \mathbf{s}[i] + \mathbf{n}[i], \tag{28}$$

where \mathbf{C}_m is a mutual coupling matrix that can be obtained from electromagnetic experiments [20]. The element $\langle \mathbf{C}_m \rangle_{ij}$ at the i -th row and the j -th column in \mathbf{C}_m represents the mutual coupling coefficient between the i -th and j -th sensors. The mutual coupling matrix is related to various factors such as antenna type, polarization, source directions, and application environment [45]–[47]. A simplified and widely adopted mutual coupling model in the literature [20], [24], [25], [48], [49] is employed, with a typical choice of $\langle \mathbf{C}_m \rangle_{ij}$ as

$$\langle \mathbf{C}_m \rangle_{ij} = \begin{cases} c_{|p_i - p_j|}, & |p_i - p_j| \leq B, \\ 0, & \text{otherwise,} \end{cases} \quad i, j \in [1, N] \tag{29}$$

where p_i, p_j are sensor positions of array \mathbb{A} , and c_k is the mutual coupling coefficient in the case that two sensors are k -separated ($|p_i - p_j| = k$). The coefficients satisfy $c_0 = 1 > |c_1| > |c_2| > \dots > |c_B| > 0 = c_{B+1}$. The magnitude of the mutual coupling coefficient is inversely proportional to sensor separations [20], [50]. In addition, the magnitude of the mutual coupling coefficient decreases rapidly with the increase of sensor separation, and a few non-zero coefficients are sufficient to describe the signal model [20], [24]. Specifically to (29), $c_k = 0$ for $k > B$ implies that the impact of k -separated mutual coupling can be ignored for $k > B$, where B is referred to as the coupling limit.

Coupling leakage is adopted to quantify the mutual coupling impact. Conceptually, the smaller the coupling leakage is, the less the mutual coupling is [20].

Definition 7: The coupling leakage of an arbitrary array is defined as [20]

$$L \triangleq \frac{\|\mathbf{C}_m - \text{diag}(\mathbf{C}_m)\|_F}{\|\mathbf{C}_m\|_F}, \tag{30}$$

where $\|\cdot\|_F$ represents the Frobenius norm, and $\text{diag}(\cdot)$ returns a diagonal matrix with the diagonal vector of the input matrix being its diagonal elements.

For existing sparse arrays based on high-order cumulants, the physical sensor spacings of the posterior subarrays are usually designed to be much larger than that of the anterior subarray to achieve large DOFs. Consider $2q$ L-NA ($q = 2$) [5] as an example, where the spacings between adjacent sensors in four subarrays are 1 for the first subarray, N_1 for the second subarray, $N_1 N_2$ for the third subarray, and $N_1 N_2 N_3$ for the fourth subarray, respectively. This design idea reduces the overall mutual coupling leakage since the mutual coupling effect between the sensors in posterior subarrays can almost be ignored due to their large spacings.

In the following proposition, the connection between the coupling leakage of the $2q$ th-O-Fractal and its generator array is derived.

Proposition 3: Consider a generator array \mathbb{G} with hole-free second-order difference co-array and a mutual coupling matrix \mathbf{C} . The coupling limit B satisfies both $B < \max(\mathbb{G})$ and $B + \max(\mathbb{G}) < M$ [14]. The $2q$ th-O-Fractal $\mathbb{E}_r^{2q} = \cup_{l=1}^q(\mathbb{E}_r(l))$ ($r \geq 1, q \geq 1$) is generated from \mathbb{G} . The coupling leakage $L_E(q)$ of \mathbb{E}_r^{2q} is

$$L_E(q) = \sqrt{\frac{N_G^{r-1} L_G^2 \|\mathbf{C}\|_F^2}{N_G^{r-1} \|\mathbf{C}\|_F^2 + (q-1)(N_G^r - 1)}} \leq L_G, \quad (31)$$

where N_G denotes the number of physical sensors in \mathbb{G} , and L_G is the coupling leakage of the generator \mathbb{G} .

Proof: See Appendix B. ■

VI. COMPARISONS WITH OTHER STRUCTURES

In this section, comparisons for sparse arrays designed for high-order difference co-array exploitation from the perspectives of robustness and mutual coupling leakage are presented. The discussions are based on the assumption of non-Gaussian sources.

A. Joint Comparisons of Robustness and Mutual Coupling

The two properties, i.e., robustness and mutual coupling, are first considered jointly, and a feasible region is formed in the two-dimensional plane as shown in Fig. 4. Array structures falling into this feasible region meet the requirements that the fragility value is smaller than 0.3 and the coupling leakage is lower than $\frac{1}{3}$ [14]. The selection of the feasible region is a trade-off between robustness and mutual coupling, and depends on requirements of practical applications.

The proposed $2q$ th-O-Fractal inherits the mentioned properties from its generator. If the selected generator with hole-free second-order difference co-array falls into the feasible region, i.e.,

$$F_G \leq 0.3, \quad L_G \leq \frac{1}{3}, \quad (32)$$

the generated $2q$ th-O-Fractal $\mathbb{E}_r^{2q} = \cup_{l=1}^q(\mathbb{E}_r(l))$ is also in the feasible region with arbitrary cumulant order q and fractal order r with

$$F_1(\mathbb{E}_r^{2q}, \mathcal{J}_{ce}) \leq F_G^r \leq 0.3, \quad L_E(q) \leq L_G \leq \frac{1}{3}, \quad (33)$$

as proved in *Proposition 2* and *Proposition 3*.

Specific examples are given to illustrate the advantages of fractal arrays in the joint design of robustness and mutual coupling. Two simple generator arrays \mathbb{G}_1 and \mathbb{S}_1 (see (26) and (27)) within the feasible region (as shown in Table I) are employed, and the $2q$ th-O-Fractal ($q = 2$ and $r = 1$) generated from \mathbb{G}_1 is

$$\mathbb{E}_1^4(\mathbb{G}_1) = \cup_{l=1}^2(\mathbb{E}_1(l)) = \{0, 1, 3, 5, 11, 13, 17, 18, 19, 20, 61, 143, 225, 471, 553, 717, 758, 799, 840\}. \quad (34)$$

The fragility and coupling leakage of $\mathbb{E}_1^4(\mathbb{G}_1)$ are 0.21 and 0.23, respectively, both falling into the feasible region.

The $2q$ th-O-Fractal ($q = 2$ and $r = 1$) generated from \mathbb{S}_1 is

$$\mathbb{E}_1^4(\mathbb{S}_1) = \cup_{l=1}^2(\mathbb{E}_1(l)) = \{0, 1, 2, 4, 7, 10, 13, 16, 18, 19, 20, 61, 102, 184, 307, 430, 553, 676, 758, 799, 840\}, \quad (35)$$

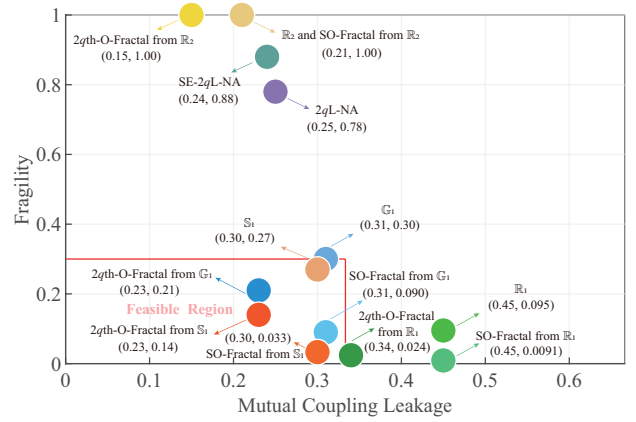


Fig. 4. Comparison of the array fragility and coupling leakage for various sparse configurations.

with its fragility and coupling leakage being 0.14 and 0.23, respectively, all within the feasible region.

Two existing sparse arrays exploiting high-order difference co-array, $2q$ L-NA and SE- $2q$ L-NA ($q = 2$), are considered, and their physical apertures are constrained to be approximately the same as that of $\mathbb{E}_1^4(\mathbb{G}_1)$ or $\mathbb{E}_1^4(\mathbb{S}_1)$. The sensor allocation strategy for $2q$ L-NA ($q = 2$) with 18 sensors is (6, 5, 5, 5) [5], and (5, 5, 4, 4) for SE- $2q$ L-NA ($q = 2$) with 16 sensors [7]. For $2q$ L-NA ($q = 2$), the fragility is 0.78 and the coupling leakage is 0.25, while the fragility and coupling leakage of SE- $2q$ L-NA ($q = 2$) are 0.88 and 0.24, respectively.

The above-mentioned arrays are drawn on a two-dimensional plane in Fig. 4. It is clear that the $2q$ th-O-Fractal arrays inherit the properties of their generators, and they are located in the feasible region with even smaller fragility and coupling leakage achieved. However, $2q$ L-NA and SE- $2q$ L-NA are not located in the feasible region since fragility and mutual coupling are not considered in their design.

Additionally, only one criterion (either low fragility or low mutual coupling) might be of interest in specific applications. If low fragility is more important, a highly robust fractal array with its fragility as low as 0.024 can be obtained by choosing ULA ($\mathbb{R}_1 = [0, 20]$) as the generator array. To achieve low mutual coupling, fractal array with coupling leakage of only 0.15 can be generated from MRA ($\mathbb{R}_2 = \{0, 1, 4, 10, 16, 18, 21, 23\}$). These generators and corresponding $2q$ th-O-Fractal arrays ($q = 2$ and $r = 1$) are also shown in Fig. 4.

The generators $\mathbb{G}_1, \mathbb{S}_1, \mathbb{R}_1$, and \mathbb{R}_2 are all designed based on the second-order difference co-array, and we have also added the SO-Fractal ($r = 2$) corresponding to the four generator arrays in Fig. 4 for comparison. Here for $r = 1$, the associated SO-Fractal is the same as its generator. Under the constraint of comparable number of uDOFs, the number of physical sensors of SO-Fractal based on the second-order difference co-array is far more than that of the $2q$ th-O-Fractal exploiting the $2q$ th-order difference co-array, e.g., 100 sensors is required for SO-Fractal from \mathbb{G}_1 to achieve a similar number of uDOFs compared with the 19-sensor $2q$ th-O-Fractal from \mathbb{G}_1 . This is consistent with the conclusion in Part I [17] that sparse arrays designed for high-order cumulants exploitation offer

many more DOFs ($\mathcal{O}(N^{2q})$ with N physical sensors) than those based on second-order difference co-arrays ($\mathcal{O}(N^2)$). Furthermore, as shown in Fig. 4, the coupling leakage of $2q$ th-O-Fractal is always smaller than that of its generator, while SO-Fractal shares the same leakage level as the generator array. The upper bound of fragility decreases with the increase of the fractal order r (see *Proposition 1* and *Proposition 2*). For the same order $r = 1$, SO-Fractal ($r = 1$) is the same as the generator, and its fragility is larger than that of the $2q$ th-O-Fractal ($q = 2$ and $r = 1$). For $r = 2$ and $r = 3$, similar conclusion can be drawn from Table I that smaller fragility is achieved by $2q$ th-O-Fractal compared with SO-Fractal based on the same generator.

B. Influence of Sensor Damage and Mutual Coupling

For the three arrays $2q$ L-NA, SE- $2q$ L-NA, and $2q$ th-O-Fractal generated from \mathbb{G}_1 ($q = 2$ and $r = 1$), sensor damage and mutual coupling are introduced in simulations to show their influence on DOA estimation. As given in Section VI-A, 18-sensor $2q$ L-NA ($q = 2$) with (6, 5, 5, 5) [5], 16-sensor SE- $2q$ L-NA ($q = 2$) with (5, 5, 4, 4) [7], and the 19-sensor $2q$ th-O-Fractal ($q = 2$ and $r = 1$) generated from \mathbb{G}_1 are included for comparison. Under the aperture constraint, these structures provide comparable numbers of consecutive lags (1799 for $2q$ L-NA, 1651 for SE- $2q$ L-NA, and 1721 for $2q$ th-O-Fractal).

For the influence of sensor damage, the input SNR and the number of snapshots are fixed at 10 dB and 4000, respectively. The SS-MUSIC method is applied to the virtual array output model for DOA estimation [5]. A total of 20 sources are uniformly distributed from -60° to 60° , and the damage to each sensor is independent. In different simulations, we assume that the sensor failure probability of each sensor is 10^{-3} , $10^{-2.75}$, $10^{-2.5}$, $10^{-2.25}$, 10^{-2} , $10^{-1.75}$, $10^{-1.5}$, $10^{-1.25}$, 10^{-1} , and $10^{-0.75}$, respectively. The root mean square error (RMSE) results of all sources are obtained through Monte Carlo simulations of 500 trials, as shown in Fig. 5, where it is clear that the proposed fractal array has better estimation accuracy compared with the other two structures due to its lower fragility, and a better performance can still be achieved for a high sensor failure probability of $10^{-1.25}$.

The total estimation error for all sources in each trial is also calculated, and a trial with a total error larger than 10 degrees is regarded as a failed detection. Fig. 6 shows the probability of successful detection for each structure under different sensor failure probabilities. It is clear that there exists substantial performance degradation for $2q$ L-NA and SE- $2q$ L-NA with the increase of the sensor failure probability, while the degradation for $2q$ th-O-Fractal is much smaller.

Mutual coupling influence on DOA estimation performance is then examined. Similar to the coupling coefficients adopted in [14], [20], [25], [51], we set $c_1 = |c_1|e^{j\pi/3}$ and $c_k = c_1/k \cdot e^{-j(k-1)\pi/8}$ for $k \in [2, B]$, while $B = 20$. The input SNR and the number of snapshots are 10 dB and 4000, respectively, and the SS-MUSIC method is employed to estimate the DOAs of 20 sources uniformly distributed from -60° to 60° . The RMSE of different array structures with respect to $|c_1|$ (ranging from 0 to 0.45 with a step size of

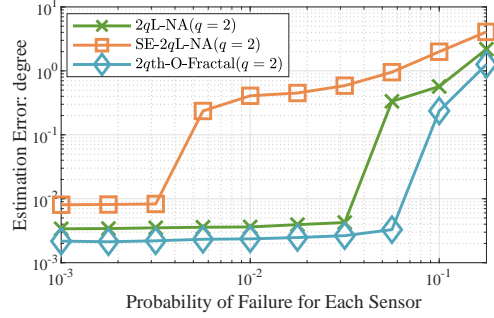


Fig. 5. RMSE with respect to varied probability of sensor failure.

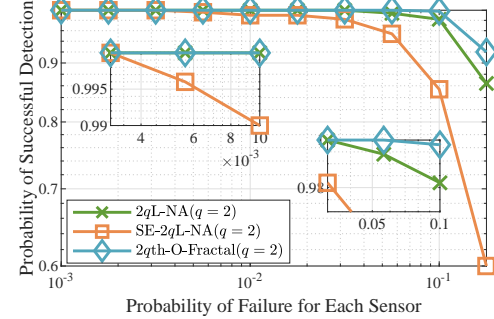


Fig. 6. Probability of successful detection with respect to varied probability of sensor failure.

0.05) are shown in Fig. 7. Similarly, the $2q$ th-O-Fractal ($q = 2$ and $r = 1$) achieves the best performance among all structures due to its lower coupling leakage. While the $2q$ th-O-Fractal ($q = 2$ and $r = 1$) achieves a good estimation performance for a strong $|c_1| = 0.3$, the others have clearly failed. According to the probability of successful detection versus the coupling coefficient (Fig. 8), the detection probability of the proposed $2q$ th-O-Fractal ($q = 2$ and $r = 1$) is higher than that of the other two structures consistently. Similar results showing that the proposed structure performs better in the presence of mutual coupling can still be obtained in simulations with changed coupling coefficient phases.

DOA estimation performance is studied to verify the impact of sensor damage and mutual coupling in resolving multiple sources. The input SNR and the number of snapshots are set as 10 dB and 5000, respectively. Consider 33 sources uniformly distributed from -60° to 60° . In Fig. 9(a)-(c), all the sparse array structures can distinguish the 33 sources successfully.

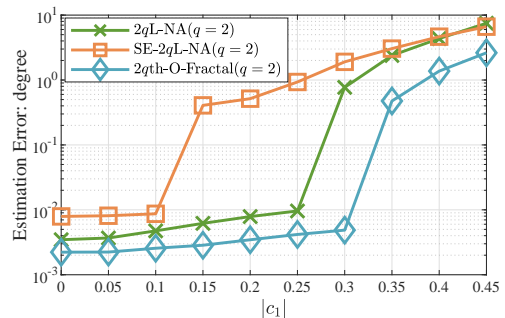


Fig. 7. RMSE with respect to varied mutual coupling coefficient.

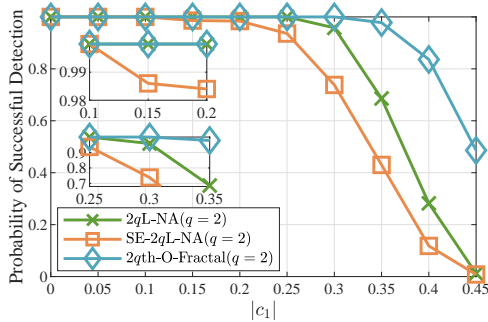


Fig. 8. Probability of successful detection with respect to varied mutual coupling coefficient.

However, if the sensor at 3 is broken for all structures, only the proposed $2q$ th-O-Fractal is capable of resolving all the sources as shown in Fig. 9(f), while the others can not (Figs. 9(d) and 9(e)).

Next, the resolution ability under mutual coupling is examined. There are 30 sources uniformly distributed from -60° to 60° . DOA estimation results are given in Fig. 10, where all 30 sources are resolved successfully by the three structures without the mutual coupling effect, as shown in Fig. 10(a)-(c). By introducing mutual coupling with $|c_1| = 0.3$, only the proposed $2q$ th-O-Fractal is able to resolve all sources as can be seen in Fig. 10(f).

Finally, we set the working frequency as 2 GHz, and planar spiral antennas with a radius of 17 mm (the antenna model is shown in Fig. 11(a)) are employed in electromagnetic simulations. By establishing models of three array structures involved with a unit spacing $d = \frac{\lambda}{3}$ to ensure severe coupling effect, the mutual coupling matrices are calculated using HFSS (High Frequency Structure Simulator), an electromagnetic simulation software. With mutual coupling matrices matched to the electromagnetic model, the DOA estimation results of the three structures are shown in Fig. 11. Obviously, only the proposed $2q$ th-O-Fractal is capable of resolving all the 9 sources, which again verifies the superior performance of the proposed structure against mutual coupling.

VII. CONCLUSION

Following our proposed fractal framework exploiting the $2q$ th-order difference co-arrays in Part I [17], here the relationship between array robustness/mutual coupling of the proposed $2q$ th-O-Fractal and its generator array was analyzed. After introducing an evaluation tool suitable for robustness analysis of array structures based on the high-order difference co-array, the fragility upper bound of $2q$ th-O-Fractal was derived as a function of the fragility of the generator array and the fractal order. Apart from increasing the fractal order, designing a robust generator array is another effective way to improve array robustness. It has been shown that, the mutual coupling leakage of $2q$ th-O-Fractal is upper bounded by that of the generator array, and reduced mutual coupling is expected if a generator array with low mutual coupling leakage is selected. Simulations demonstrated that, $2q$ th-O-Fractal with both small fragility and low mutual coupling leakage can be flexibly generated, and better performance can be achieved than $2q$ L-NA

and SE- $2q$ L-NA in the presence of random sensor damage and mutual coupling effect. Furthermore, it has also been shown that, compared with the SO-Fractal structure exploiting the second-order difference co-array, smaller fragility and lower mutual coupling leakage can be achieved by the proposed $2q$ th-O-Fractal generated from the same generator and fractal order.

Combining the results in Part I and Part II, we conclude that the proposed framework provides an effective approach to sparse array design with several important properties inherited from its prototype generator array. By optimizing the generator array according to given criteria (i.e., large consecutive difference co-array, hole-free difference co-array, closed-form sensor positions, robustness and economy, and low mutual coupling), the associated $2q$ th-O-Fractal can be easily obtained incorporating multiple properties of interest.

APPENDIX A PROOF OF LEMMA 2

We prove the lemma by mathematical induction.

For $q = 1$, the $2q$ th-O-Fractal \mathbb{E}_r^{2q} becomes the original SO-Fractal, so the sensors in $\mathbb{I}_r^{2q} = \mathbb{I}_{r(1)}$ are all inessential.

For $q = p$, provided that the sensors in $\mathbb{I}_r^{2p} = \bigcup_{l=1}^p \mathbb{I}_{r(l)}$ are all inessential with respect to $\mathbb{U}_{2p}(\mathbb{E}_r)$, for $q = p + 1$, the criterion for judging a sensor e as an inessential sensor with respect to $\mathbb{U}_{2p+2}(\mathbb{E}_r)$ (*Definition 2*) is

$$\overline{\mathbb{D}}_{2p+2(e)} \supseteq \mathbb{U}_{2p+2}(\mathbb{E}_r), \quad (36)$$

$$\overline{\mathbb{D}}_{2p+2(e)} = \left\{ \sum_{k=1}^{p+1} (\mu_{2k} - \mu_{2k-1}) \mid \mu \in \mathbb{E}_r^{2p+2} \setminus \{e\} \right\}, \quad (37)$$

where $\overline{\mathbb{D}}_{2p+2(e)}$ is the $(2p+2)$ th-order difference co-array of \mathbb{E}_r^{2p+2} after removing the sensor e .

Since the composition of $\overline{\mathbb{D}}_{2p+2(e)}$ is extremely complicated, the core composition Φ_{2p+2} in *Definition 6* is introduced to assist the analysis.

If a sensor e is removed during the construction of the core composition Φ_{2p+2} , it will lead to a new composition $\overline{\Phi}_{2p+2(e)}$ that may be partially defective. Since $\mathbb{D}_{2p+2} \supseteq \Phi_{2p+2}$, $\overline{\mathbb{D}}_{2p+2(e)} \supseteq \overline{\Phi}_{2p+2(e)}$ always holds. If $\overline{\Phi}_{2p+2(e)}$ can still completely contain $\mathbb{U}_{2p+2}(\mathbb{E}_r)$, then according to the transitivity, one can derive

$$\overline{\mathbb{D}}_{2p+2(e)} \supseteq \overline{\Phi}_{2p+2(e)} \supseteq \mathbb{U}_{2p+2}(\mathbb{E}_r), \quad (38)$$

which means that sensor e is an inessential sensor. Next, we use the ideas outlined above to prove the sensors in $\mathbb{I}_r^{2p+2} = \bigcup_{l=1}^{p+1} \mathbb{I}_{r(l)}$ are all inessential with respect to $\mathbb{U}_{2p+2}(\mathbb{E}_r)$.

First, a suitable core composition Φ_{2p+2} is found in deriving the closed-form number of uDOFs guaranteed by the $2q$ th-O-Fractal (Proposition 1 in Part I [17]). It consists of three parts,

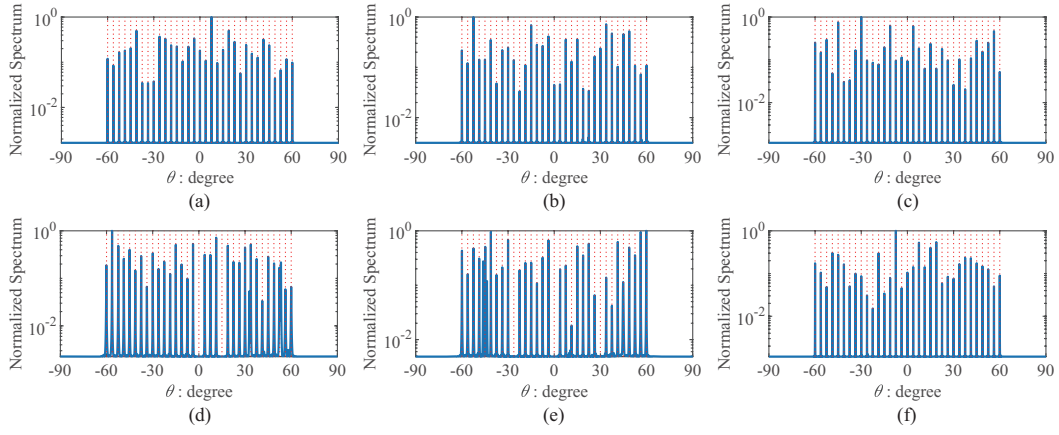


Fig. 9. DOA estimation results of different array structures with/without sensor damage. Results of (a) $2qL$ -NA ($q = 2$), (b) SE- $2qL$ -NA ($q = 2$), (c) $2q$ th-O-Fractal ($q = 2$ and $r = 1$), (d) $2qL$ -NA ($q = 2$) without sensor at 3, (e) SE- $2qL$ -NA ($q = 2$) without sensor at 3, (f) $2q$ th-O-Fractal ($q = 2$ and $r = 1$) without sensor at 3.

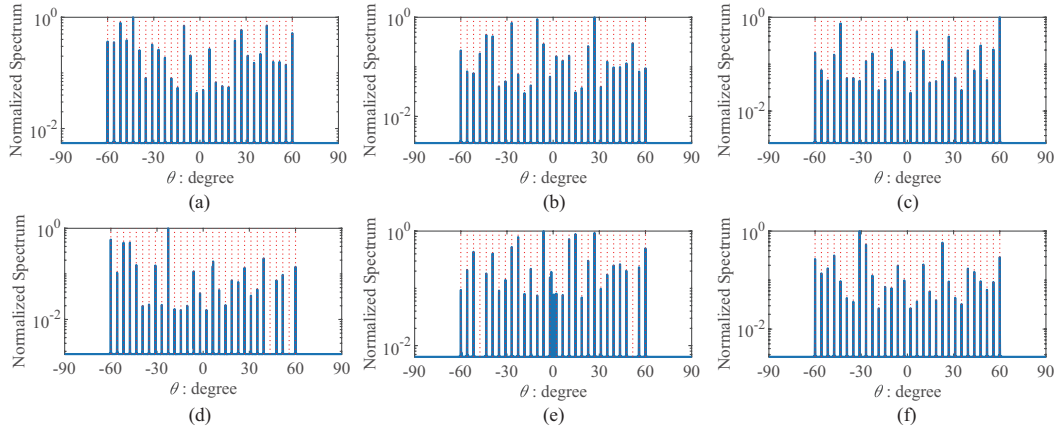


Fig. 10. DOA estimation results of different array structures with/without mutual coupling. Results of (a) $2qL$ -NA ($q = 2$) without mutual coupling, (b) SE- $2qL$ -NA ($q = 2$) without mutual coupling, (c) $2q$ th-O-Fractal ($q = 2$ and $r = 1$) without mutual coupling, (d) $2qL$ -NA ($q = 2$) with the coupling coefficient $|c_1| = 0.3$, (e) SE- $2qL$ -NA ($q = 2$) with the coupling coefficient $|c_1| = 0.3$, (f) $2q$ th-O-Fractal ($q = 2$ and $r = 1$) with the coupling coefficient $|c_1| = 0.3$.

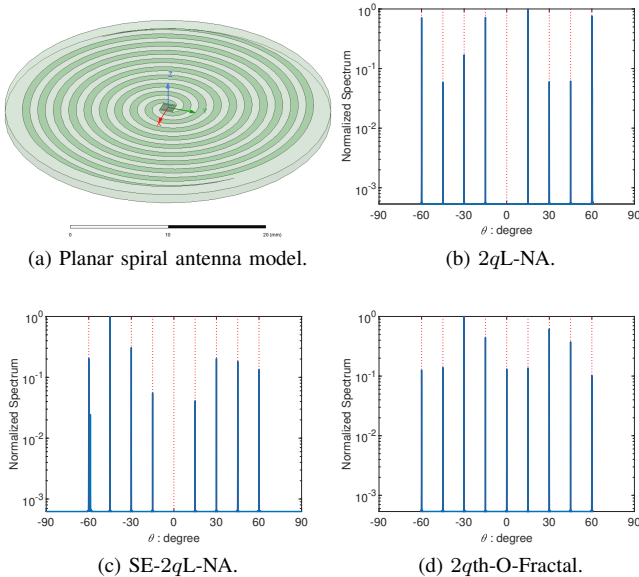


Fig. 11. Planar spiral antenna model and DOA estimation results of different array structures with severe mutual coupling.

expressed as

$$\begin{aligned}
 \Phi_{2p+2} &= \Phi'_{2p+2} \cup \Phi''_{2p+2} \cup \Phi'''_{2p+2}, \\
 \Phi'_{2p+2} &= \left\{ (\mu_{2p+2} - \mu_{2p+1}) + \sum_{k=1}^p (\mu_{2k} - \mu_{2k-1}) \mid \right. \\
 &\quad \left. \mu_{2p+1}, \mu_{2p+2} \in \mathbb{E}_{r(p+1)}, \mu_1, \mu_2, \dots, \mu_{2p} \in \mathbb{E}_r^{2p} \right\}, \\
 \Phi''_{2p+2} &= \left\{ (\mu_{2p+2} - \mu_{2p+1}) + \sum_{k=1}^p (\mu_{2k} - \mu_{2k-1}) \mid \right. \\
 &\quad \left. \mu_{2p+2} = f_{r(i)}T_{p+1} + m_{p+1}, \mu_{2p+1} = f_{r(j)}T_p + m_p, \right. \\
 &\quad \left. \mu_1, \mu_2, \dots, \mu_{2p} \in \mathbb{E}_r^{2p} \right\}, \\
 \Phi'''_{2p+2} &= \left\{ (\mu_{2p+1} - \mu_{2p+2}) + \sum_{k=1}^p (\mu_{2k} - \mu_{2k-1}) \mid \right. \\
 &\quad \left. \mu_{2p+2} = f_{r(i)}T_{p+1} + m_{p+1}, \mu_{2p+1} = f_{r(j)}T_p + m_p, \right. \\
 &\quad \left. \mu_1, \mu_2, \dots, \mu_{2p} \in \mathbb{E}_r^{2p} \right\}.
 \end{aligned} \tag{39}$$

Then, the following results related to the three parts in the core combination Φ_{2p+2} can be derived, which are (Proposition 1

in Part I [17])

$$\begin{aligned}\Phi'_{2p+2} &\supseteq \left[-\frac{T_{p+1}M^r-1}{2}, \frac{T_{p+1}M^r-1}{2} \right], \\ \Phi''_{2p+2} &\supseteq \left[\frac{T_{p+1}(M^r-2)+T_p(M^r-1)+1}{2}, \frac{T_{p+1}M^r+T_p(M^r-1)-1}{2} \right], \\ \Phi'''_{2p+2} &\supseteq \left[-\frac{T_{p+1}M^r+T_p(M^r-1)-1}{2}, -\frac{T_{p+1}(M^r-2)+T_p(M^r-1)+1}{2} \right],\end{aligned}$$

and one has

$$\Phi_{2p+2} = \Phi'_{2p+2} \cup \Phi''_{2p+2} \cup \Phi'''_{2p+2} \supseteq \mathbb{U}_{2p+2}(\mathbb{E}_r). \quad (40)$$

Next, the elements in \mathbb{I}_r^{2p+2} are divided into two parts, i.e., $\mathbb{I}_{r(p+1)}$ and $\mathbb{I}_r^{2p} = \bigcup_{l=1}^p \mathbb{I}_{r(l)}$, and their essentialness is discussed separately. Note that the sensors in $\mathbb{I}_{r(p+1)}$ belong to the $(p+1)$ -th subarray $\mathbb{E}_{r(p+1)}$ of \mathbb{E}_r^{2p+2} , while $\mathbb{I}_{r(p)} \subseteq \mathbb{E}_r^{2p}$. Since the second-order difference co-array of the generator array is hole-free, the second-order difference co-array (denoted by \mathbb{D}_2) of SO-Fractal $\mathbb{E}_{r(1)}$ is also hole-free with $\mathbb{D}_2 = \mathbb{U}_{2p}(\mathbb{E}_r)$. Therefore, the largest consecutive lag in \mathbb{D}_2 is

$$\max(\mathbb{E}_{r(1)}) - \min(\mathbb{E}_{r(1)}) = \frac{M^r - 1}{2}, \quad (41)$$

which implies $f_{r(i)} = \max(\mathbb{E}_{r(1)})$ and $f_{r(j)} = \min(\mathbb{E}_{r(1)})$.

According to Lemma 2 of [18], the leftmost element ($\min(\mathbb{E}_{r(1)})$) and the rightmost element ($\max(\mathbb{E}_{r(1)})$) are both essential to \mathbb{D}_2 , leading to $f_{r(i)}T_{p+1} + m_{p+1} \notin \mathbb{I}_r^{2p+2}$ and $f_{r(j)}T_p + m_p \notin \mathbb{I}_r^{2p+2}$.

If a sensor $e_{i1} \in \mathbb{I}_{r(p+1)}$ is removed in constructing the core composition Φ_{2p+2} , $\bar{\Phi}_{2p+2}(e_{i1})$ is obtained with

$$\begin{aligned}\bar{\Phi}_{2p+2}(e_{i1}) &= \bar{\Phi}'_{2p+2}(e_{i1}) \cup \bar{\Phi}''_{2p+2}(e_{i1}) \cup \bar{\Phi}'''_{2p+2}(e_{i1}), \quad (42) \\ \bar{\Phi}'_{2p+2}(e_{i1}) &= \left\{ (\mu_{2p+2} - \mu_{2p+1}) + \sum_{k=1}^p (\mu_{2k} - \mu_{2k-1}) \mid \right. \\ &\quad \left. \mu_{2p+1}, \mu_{2p+2} \in \mathbb{E}_{r(p+1)} \setminus \{e_{i1}\}, \mu_1, \dots, \mu_{2p} \in \mathbb{E}_r^{2p} \right\}, \\ \bar{\Phi}''_{2p+2}(e_{i1}) &= \bar{\Phi}''_{2p+2}, \quad \bar{\Phi}'''_{2p+2}(e_{i1}) = \bar{\Phi}'''_{2p+2}.\end{aligned}$$

Since

$$\begin{aligned}\bar{\Phi}'_{2p+2}(e_{i1}) &\supseteq \left\{ (\mu_{2p+2} - \mu_{2p+1}) + \mu' \mid \mu_{2p+1}, \mu_{2p+2} \right. \\ &\quad \left. \in \mathbb{E}_{r(p+1)} \setminus \{e_{i1}\}, \mu' \in \mathbb{U}_{2p}(\mathbb{E}_r) \right\} \\ &= \left\{ \mu'' T_{p+1} + \mu' \mid \mu'' \in \mathbb{D}_2, \mu' \in \mathbb{U}_{2p}(\mathbb{E}_r) \right\} \\ &= \left[-\frac{T_{p+1}M^r-1}{2}, \frac{T_{p+1}M^r-1}{2} \right], \quad (43)\end{aligned}$$

then, $\bar{\mathbb{D}}_{2p+2}(e_{i1}) \supseteq \bar{\Phi}_{2p+2}(e_{i1}) \supseteq \mathbb{U}_{2p+2}(\mathbb{E}_r)$ can be derived, which implies that any sensor $e_{i1} \in \mathbb{I}_{r(p+1)}$ is inessential with respect to $\mathbb{U}_{2p+2}(\mathbb{E}_r)$.

If a sensor $e_{i2} \in \mathbb{I}_r^{2p}$ is removed in constructing Φ_{2p+2} ,

$\bar{\Phi}_{2p+2}(e_{i2})$ is obtained by

$$\begin{aligned}\bar{\Phi}_{2p+2}(e_{i2}) &= \bar{\Phi}'_{2p+2}(e_{i2}) \cup \bar{\Phi}''_{2p+2}(e_{i2}) \cup \bar{\Phi}'''_{2p+2}(e_{i2}), \quad (44) \\ \bar{\Phi}'_{2p+2}(e_{i2}) &= \left\{ (\mu_{2p+2} - \mu_{2p+1}) + \sum_{k=1}^p (\mu_{2k} - \mu_{2k-1}) \mid \right. \\ &\quad \left. \mu_{2p+1}, \mu_{2p+2} \in \mathbb{E}_{r(p+1)}, \mu_1, \dots, \mu_{2p} \in \mathbb{E}_r^{2p} \setminus \{e_{i2}\} \right\}, \\ \bar{\Phi}''_{2p+2}(e_{i2}) &= \left\{ (\mu_{2p+2} - \mu_{2p+1}) + \sum_{k=1}^p (\mu_{2k} - \mu_{2k-1}) \mid \right. \\ &\quad \left. \mu_{2p+2} = f_{r(i)}T_{p+1} + m_{p+1}, \mu_{2p+1} = f_{r(j)}T_p + m_p, \right. \\ &\quad \left. \mu_1, \mu_2, \dots, \mu_{2p} \in \mathbb{E}_r^{2p} \setminus \{e_{i2}\} \right\}, \\ \bar{\Phi}'''_{2p+2}(e_{i2}) &= \left\{ (\mu_{2p+1} - \mu_{2p+2}) + \sum_{k=1}^p (\mu_{2k} - \mu_{2k-1}) \mid \right. \\ &\quad \left. \mu_{2p+2} = f_{r(i)}T_{p+1} + m_{p+1}, \mu_{2p+1} = f_{r(j)}T_p + m_p, \right. \\ &\quad \left. \mu_1, \mu_2, \dots, \mu_{2p} \in \mathbb{E}_r^{2p} \setminus \{e_{i2}\} \right\}.\end{aligned}$$

According to the assumption that all sensors in $\mathbb{I}_r^{2p} = \bigcup_{l=1}^p \mathbb{I}_{r(l)}$ are all inessential with respect to $\mathbb{U}_{2p}(\mathbb{E}_r)$, one has

$$\left\{ \sum_{k=1}^p (\mu_{2k} - \mu_{2k-1}) \mid \mu_1, \dots, \mu_{2p} \in \mathbb{E}_r^{2p} \setminus \{e_{i2}\} \right\} \supseteq \mathbb{U}_{2p}(\mathbb{E}_r).$$

Therefore,

$$\begin{aligned}\bar{\Phi}'_{2p+2}(e_{i2}) &\supseteq \left\{ (\mu_{2p+2} - \mu_{2p+1}) + \mu' \mid \mu_{2p+1}, \mu_{2p+2} \right. \\ &\quad \left. \in \mathbb{E}_{r(p+1)}, \mu' \in \mathbb{U}_{2p}(\mathbb{E}_r) \right\}, \\ \bar{\Phi}''_{2p+2}(e_{i2}) &\supseteq \left\{ (\mu_{2p+2} - \mu_{2p+1}) + \mu' \mid \mu_{2p+2} = f_{r(i)}T_{p+1} + \right. \\ &\quad \left. m_{p+1}, \mu_{2p+1} = f_{r(j)}T_p + m_p, \mu' \in \mathbb{U}_{2p}(\mathbb{E}_r) \right\}, \\ \bar{\Phi}'''_{2p+2}(e_{i2}) &\supseteq \left\{ (\mu_{2p+1} - \mu_{2p+2}) + \mu' \mid \mu_{2p+2} = f_{r(i)}T_{p+1} + \right. \\ &\quad \left. m_{p+1}, \mu_{2p+1} = f_{r(j)}T_p + m_p, \mu' \in \mathbb{U}_{2p}(\mathbb{E}_r) \right\},\end{aligned}$$

and $\bar{\mathbb{D}}_{2p+2}(e_{i2}) \supseteq \bar{\Phi}_{2p+2}(e_{i2}) \supseteq \mathbb{U}_{2p+2}(\mathbb{E}_r)$, which implies any sensor $e_{i2} \in \mathbb{I}_r^{2p}$ is inessential to $\mathbb{U}_{2p+2}(\mathbb{E}_r)$.

This completes the proof that all sensors in \mathbb{I}_r^{2q} are inessential with respect to $\mathbb{U}_{2q}(\mathbb{E}_r)$.

APPENDIX B PROOF OF PROPOSITION 3

First, since there is always a shared sensor between adjacent subarrays of the $2q$ th-O-Fractal, it is necessary to clarify the position of the shared sensors in order to analyze the mutual coupling effect. Due to the property of hole-free second-order difference co-array of \mathbb{G} , we obtain $f_{r(j)} = \min(\mathbb{E}_{r(1)})$ and $f_{r(i)} = \max(\mathbb{E}_{r(1)})$. The position of the sensor shared by subarrays $\mathbb{E}_{r(p+1)}$ and $\mathbb{E}_{r(p)}$ is

$$\begin{aligned}f_{r(j)} \cdot T_{p+1} + m_{p+1} &= \min(\mathbb{E}_{r(1)})T_{p+1} + m_{p+1} \\ &= \min(\mathbb{E}_{r(p+1)}) = f_{r(i)} \cdot T_p + m_p \\ &= \max(\mathbb{E}_{r(1)})T_p + m_p = \max(\mathbb{E}_{r(p)}).\end{aligned}$$

As a result, the leftmost element of the subarray $\mathbb{E}_{r(p+1)}$ ($p \geq 1$) is also the rightmost element of the anterior subarray $\mathbb{E}_{r(p)}$.

Next, we analyze the $N(q) \times N(q)$ mutual coupling matrix \mathbf{C}_m of the $2q$ th-O-Fractal \mathbb{E}_r^{2q} . According to (29), $\langle \mathbf{C}_m \rangle_{ij}$ at

the i -th row and j -th column of \mathbf{C}_m is related to the interval between the i -th sensor e_i and the j -th sensor e_j in \mathbb{E}_r^{2q} . All possible values of e_i and e_j are discussed as follows.

- If $e_i \in \mathbb{E}_{r(1)}$ and $e_j \in \mathbb{E}_{r(1)}$, this case is similar to that discussed in Theorem 7 of [14], and then $\langle \mathbf{C}_m \rangle_{ij} = \langle \mathbf{C}_{E1} \rangle_{ij}$, with the $N_G^r \times N_G^r$ matrix \mathbf{C}_{E1} being

$$\mathbf{C}_{E1} = \begin{bmatrix} \mathbf{C} & \mathbf{0} & \cdots & \mathbf{0} \\ \mathbf{0} & \mathbf{C} & \ddots & \vdots \\ \vdots & \ddots & \ddots & \mathbf{0} \\ \mathbf{0} & \cdots & \mathbf{0} & \mathbf{C} \end{bmatrix}. \quad (45)$$

- If $e_i \in \mathbb{E}_{r(1)}$ and $e_j \in \cup_{l=3}^q (\mathbb{E}_{r(l)} \cup \mathbb{E}_{r(2)} \setminus \min(\mathbb{E}_{r(2)}))$, then,

$$\begin{aligned} |e_i - e_j| &= e_j - e_i \\ &\geq \min(\mathbb{E}_{r(2)} \setminus \min(\mathbb{E}_{r(2)})) - \max(\mathbb{E}_{r(1)}) \\ &= \min(\mathbb{E}_{r(2)} \setminus \min(\mathbb{E}_{r(2)})) - \min(\mathbb{E}_{r(2)}) \\ &\geq T_2 = M^r > B. \end{aligned} \quad (46)$$

- If $e_i \in \mathbb{E}_{r(p)} \setminus \min(\mathbb{E}_{r(p)})$ and $e_j \in \mathbb{E}_{r(p)} \setminus \min(\mathbb{E}_{r(p)})$ ($p \geq 2$), then $|e_i - e_j|$ satisfies

$$|e_i - e_j| \geq T_p \geq T_2 > B. \quad (47)$$

- If $e_i \in \mathbb{E}_{r(p)} \setminus \min(\mathbb{E}_{r(p)})$ and $e_j \in \cup_{l=p+2}^q (\mathbb{E}_{r(l)} \cup \mathbb{E}_{r(p+1)} \setminus \min(\mathbb{E}_{r(p+1)}))$ ($p \geq 2$), the interval between e_i and e_j holds

$$\begin{aligned} |e_i - e_j| &= e_j - e_i \\ &\geq \min(\mathbb{E}_{r(p+1)} \setminus \min(\mathbb{E}_{r(p+1)})) - \max(\mathbb{E}_{r(p)}) \\ &= \min(\mathbb{E}_{r(p+1)} \setminus \min(\mathbb{E}_{r(p+1)})) - \min(\mathbb{E}_{r(p+1)}) \\ &\geq T_{p+1} > T_2 > B. \end{aligned} \quad (48)$$

- If $e_i \in \mathbb{E}_{r(p)} \setminus \min(\mathbb{E}_{r(p)})$, $e_j \in \cup_{l=1}^{p-1} (\mathbb{E}_{r(l)})$ and $p \geq 2$, the following can be derived

$$\begin{aligned} |e_i - e_j| &= e_i - e_j \\ &\geq \min(\mathbb{E}_{r(p)} \setminus \min(\mathbb{E}_{r(p)})) - \max(\mathbb{E}_{r(p-1)}) \\ &= \min(\mathbb{E}_{r(p)} \setminus \min(\mathbb{E}_{r(p)})) - \min(\mathbb{E}_{r(p)}) \\ &\geq T_p \geq T_2 > B. \end{aligned} \quad (49)$$

Due to the self-similarity of the proposed structure, the coupling coefficients between physical sensors within each subarray form a block diagonal matrix. Based on the above discussions, the spacing between any sensors from different subarrays (after stripping the shared sensor) is greater than the coupling limit B , and thus the corresponding coupling coefficient is 0. Therefore, according to (45) to (49), the block diagonal form of \mathbf{C}_m can be derived as

$$\mathbf{C}_m = \begin{bmatrix} \mathbf{C}_{E1} & \mathbf{0} & \cdots & \mathbf{0} \\ \mathbf{0} & \mathbf{C}_{E2} & \ddots & \vdots \\ \vdots & \ddots & \ddots & \mathbf{0} \\ \mathbf{0} & \cdots & \mathbf{0} & \mathbf{C}_{Eq} \end{bmatrix} \quad (50)$$

where \mathbf{C}_{Ep} ($p \in [2, q]$) with the size of $(N_G^r - 1) \times (N_G^r - 1)$ is expressed as

$$\mathbf{C}_{Ep} = \begin{bmatrix} 1 & 0 & \cdots & 0 \\ 0 & 1 & \ddots & \vdots \\ \vdots & \ddots & \ddots & 0 \\ 0 & \cdots & 0 & 1 \end{bmatrix}. \quad (51)$$

Substituting (50) into the definition of coupling leakage yields

$$\begin{aligned} L_E(q) &= \frac{\|\mathbf{C}_m - \text{diag}(\mathbf{C}_m)\|_F}{\|\mathbf{C}_m\|_F} \\ &= \sqrt{\frac{\|\mathbf{C}_{E1} - \text{diag}(\mathbf{C}_{E1})\|_F^2}{\|\mathbf{C}_{E1}\|_F^2 + (q-1)(N_G^r - 1)}}. \end{aligned} \quad (52)$$

Since (Theorem 7 in [14])

$$\begin{aligned} \frac{\|\mathbf{C}_{E1} - \text{diag}(\mathbf{C}_{E1})\|_F}{\|\mathbf{C}_{E1}\|_F} &= L_G, \\ \|\mathbf{C}_{E1} - \text{diag}(\mathbf{C}_{E1})\|_F &= \|\mathbf{I}_{N'} \otimes (\mathbf{C} - \text{diag}(\mathbf{C}))\|_F \\ &= \sqrt{N'} \|\mathbf{C} - \text{diag}(\mathbf{C})\|_F, \\ \|\mathbf{C}_{E1}\|_F &= \|\mathbf{I}_{N'} \otimes \mathbf{C}\|_F \\ &= \sqrt{N'} \|\mathbf{C}\|_F, \end{aligned} \quad (53)$$

with $N' = N_G^{r-1}$, one can derive

$$\begin{aligned} L_E(q) &= \sqrt{\frac{\|\mathbf{C}_{E1} - \text{diag}(\mathbf{C}_{E1})\|_F^2}{\|\mathbf{C}_{E1}\|_F^2 + (q-1)(N_G^r - 1)}} \\ &= \sqrt{\frac{N_G^{r-1} L_G^2 \|\mathbf{C}\|_F^2}{N_G^{r-1} \|\mathbf{C}\|_F^2 + (q-1)(N_G^r - 1)}} \\ &\leq \sqrt{\frac{N_G^{r-1} L_G^2 \|\mathbf{C}\|_F^2}{N_G^{r-1} \|\mathbf{C}\|_F^2}} = L_G, \end{aligned} \quad (54)$$

which completes the proof.

REFERENCES

- [1] P. P. Vaidyanathan and P. Pal, "Sparse sensing with co-prime samplers and arrays," *IEEE Trans. Signal Process.*, vol. 59, no. 2, pp. 573–586, Feb. 2011.
- [2] P. Pal and P. P. Vaidyanathan, "Nested arrays: A novel approach to array processing with enhanced degrees of freedom," *IEEE Trans. Signal Process.*, vol. 58, no. 8, pp. 4167–4181, 2010.
- [3] Q. Shen, W. Liu, W. Cui, and S. Wu, "Underdetermined DOA estimation under the compressive sensing framework: A review," *IEEE Access*, vol. 4, pp. 8865–8878, 2016.
- [4] Y. Liang, W. Cui, Q. Shen, W. Liu, and S. Wu, "Cramér-Rao bound analysis of underdetermined wideband DOA estimation under the sub-band model via frequency decomposition," *IEEE Trans. Signal Process.*, vol. 69, pp. 4132–4148, 2021.
- [5] P. Pal and P. P. Vaidyanathan, "Multiple level nested array: An efficient geometry for 2qth order cumulant based array processing," *IEEE Trans. Signal Process.*, vol. 60, no. 3, pp. 1253–1269, Mar. 2012.
- [6] A. Moffet, "Minimum-redundancy linear arrays," *IEEE Trans. Antennas Propagat.*, vol. 16, no. 2, pp. 172–175, Mar. 1968.
- [7] Q. Shen, W. Liu, W. Cui, S. Wu, and P. Pal, "Simplified and enhanced multiple level nested arrays exploiting high-order difference co-arrays," *IEEE Trans. Signal Process.*, vol. 67, no. 13, pp. 3502–3515, Jul. 2019.
- [8] B. Porat and B. Friedlander, "Direction finding algorithms based on high-order statistics," *IEEE Trans. Signal Process.*, vol. 39, no. 9, pp. 2016–2024, Sep. 1991.
- [9] C. Nikias and J. Mendel, "Signal processing with higher-order spectra," *IEEE Signal Process. Mag.*, vol. 10, no. 3, pp. 10–37, Jul. 1993.

- [10] M. Dogan and J. Mendel, "Applications of cumulants to array processing—Part I: Aperture extension and array calibration," *IEEE Trans. Signal Process.*, vol. 43, no. 5, pp. 1200–1216, May 1995.
- [11] E. Gonen and J. Mendel, "Applications of cumulants to array processing—Part VI: Polarization and direction of arrival estimation with minimally constrained arrays," *IEEE Trans. Signal Process.*, vol. 47, no. 9, pp. 2589–2592, Sep. 1999.
- [12] P. Chevalier, L. Albera, A. Ferreol, and P. Comon, "On the virtual array concept for higher order array processing," *IEEE Trans. Signal Process.*, vol. 53, no. 4, pp. 1254–1271, Apr. 2005.
- [13] P. Chevalier, A. Ferreol, and L. Albera, "High-resolution direction finding from higher order statistics: The $2q$ -MUSIC algorithm," *IEEE Trans. Signal Process.*, vol. 54, no. 8, pp. 2986–2997, Aug. 2006.
- [14] R. Cohen and Y. C. Eldar, "Sparse array design via fractal geometries," *IEEE Trans. Signal Process.*, vol. 68, pp. 4797–4812, 2020.
- [15] —, "Sparse fractal array design with increased degrees of freedom," in *Proc. IEEE Int. Conf. Acoust., Speech, Signal Process.*, May 2019, pp. 4195–4199.
- [16] C.-L. Liu and P. P. Vaidyanathan, "Maximally economic sparse arrays and Cantor arrays," in *Proc. IEEE Int. Workshop Comput. Advances MultiSensor Adaptive Process.*, Dec. 2017, pp. 1–5.
- [17] Z. Yang, Q. Shen, W. Liu, Y. C. Eldar, and W. Cui, "High-order cumulants based sparse array design via fractal geometries—Part I: Structures and DOFs," *IEEE Trans. Signal Process.*, submitted.
- [18] C.-L. Liu and P. P. Vaidyanathan, "Robustness of difference coarrays of sparse arrays to sensor failures—Part I: A theory motivated by coarray MUSIC," *IEEE Trans. Signal Process.*, vol. 67, no. 12, pp. 3213–3226, Jun. 2019.
- [19] T. Svantesson, "Modeling and estimation of mutual coupling in a uniform linear array of dipoles," in *Proc. IEEE Int. Conf. Acoust., Speech, Signal Process.*, 1999, pp. 2961–2964.
- [20] C.-L. Liu and P. P. Vaidyanathan, "Super nested arrays: Linear sparse arrays with reduced mutual coupling—Part I: Fundamentals," *IEEE Trans. Signal Process.*, vol. 64, no. 15, pp. 3997–4012, Aug. 2016.
- [21] S. Qin and Y. D. Zhang, "Generalized coprime array configurations for direction-of-arrival estimation," *IEEE Trans. Signal Process.*, vol. 63, no. 6, pp. 1377–1390, Mar. 2015.
- [22] C.-L. Liu and P. P. Vaidyanathan, "Super nested arrays: Linear sparse arrays with reduced mutual coupling—Part II: High-order extensions," *IEEE Trans. Signal Process.*, vol. 64, no. 16, pp. 4203–4217, Aug. 2016.
- [23] J. Liu, Y. Zhang, Y. Lu, S. Ren, and S. Cao, "Augmented nested arrays with enhanced DOF and reduced mutual coupling," *IEEE Trans. Signal Process.*, vol. 65, no. 21, pp. 5549–5563, Nov. 2017.
- [24] J. Shi, G. Hu, X. Zhang, and H. Zhou, "Generalized nested array: Optimization for degrees of freedom and mutual coupling," *IEEE Commun. Lett.*, vol. 22, no. 6, pp. 1208–1211, Jun. 2018.
- [25] A. Raza, W. Liu, and Q. Shen, "Thinned coprime array for second-order difference co-array generation with reduced mutual coupling," *IEEE Trans. Signal Process.*, vol. 67, no. 8, pp. 2052–2065, Apr. 2019.
- [26] W. Zheng, X. Zhang, Y. Wang, J. Shen, and B. Champagne, "Padded coprime arrays for improved DOA estimation: Exploiting hole representation and filling strategies," *IEEE Trans. Signal Process.*, vol. 68, pp. 4597–4611, 2020.
- [27] C.-L. Liu and P. P. Vaidyanathan, "Robustness of difference coarrays of sparse arrays to sensor failures—Part II: Array geometries," *IEEE Trans. Signal Process.*, vol. 67, no. 12, pp. 3227–3242, Jun. 2019.
- [28] D. Zhu, S. Wang, and G. Li, "Multiple-fold redundancy arrays with robust difference coarrays: Fundamental and analytical design method," *IEEE Trans. Antennas Propagat.*, vol. 69, no. 9, pp. 5570–5584, Sep. 2021.
- [29] C. Zhou, Y. Gu, S. He, and Z. Shi, "A robust and efficient algorithm for coprime array adaptive beamforming," *IEEE Trans. Veh. Technol.*, vol. 67, no. 2, pp. 1099–1112, Feb. 2018.
- [30] H. Dai, W. Shen, L. Ding, S. Gong, and J. An, "Subarray partition algorithms for RIS-aided MIMO communications," *IEEE Internet Things J.*, 2022.
- [31] W. Hao, G. Sun, M. Zeng, Z. Chu, Z. Zhu, O. A. Dobre, and P. Xiao, "Robust design for intelligent reflecting surface-assisted MIMO-OFDMA terahertz IoT networks," *IEEE Internet Things J.*, vol. 8, no. 16, pp. 13 052–13 064, Aug. 2021.
- [32] A. Alexiou and A. Manikas, "Investigation of array robustness to sensor failure," *Journal of the Franklin Institute*, vol. 342, no. 3, pp. 255–272, May 2005.
- [33] M. Carlin, G. Oliveri, and A. Massa, "On the robustness to element failures of linear ADS-thinned arrays," *IEEE Trans. Antennas Propagat.*, vol. 59, no. 12, pp. 4849–4853, Dec. 2011.
- [34] T. Peters, "A conjugate gradient-based algorithm to minimize the side-lobe level of planar arrays with element failures," *IEEE Trans. Antennas Propagat.*, vol. 39, no. 10, pp. 1497–1504, Oct. 1991.
- [35] B. Sun, C. Wu, J. Shi, H.-L. Ruan, and W.-Q. Ye, "Direction-of-arrival estimation under array sensor failures with ULA," *IEEE Access*, vol. 8, pp. 26 445–26 456, 2020.
- [36] C.-L. Liu and P. Vaidyanathan, "Novel algorithms for analyzing the robustness of difference coarrays to sensor failures," *Signal Process.*, vol. 171, p. 107517, Jun. 2020.
- [37] D. Zhu and G. Li, "Robust sparse arrays with multiple-fold redundant difference coarrays," in *IEEE Int. Conf. Signal, Inf. Data Process.*, Dec. 2019, pp. 1–4.
- [38] C.-L. Liu and P. P. Vaidyanathan, "Comparison of sparse arrays from viewpoint of coarray stability and robustness," in *Proc. IEEE Sensor Array Multichannel Signal Process. Workshop (SAM)*, Jul. 2018, pp. 36–40.
- [39] —, "Optimizing minimum redundancy arrays for robustness," in *Proc. IEEE Asilomar Conf. Signals, Syst., Comput.*, Oct. 2018, pp. 79–83.
- [40] —, "Composite Singer arrays with hole-free coarrays and enhanced robustness," in *Proc. IEEE Int. Conf. Acoust., Speech, Signal Process.*, May 2019, pp. 4120–4124.
- [41] C.-L. Liu, "A general framework for the robustness of structured difference coarrays to element failures," in *Proc. IEEE Sensor Array Multichannel Signal Process. Workshop (SAM)*, Jun. 2020, pp. 1–5.
- [42] H. Wu, Q. Shen, W. Cui, and W. Liu, "DOA estimation with nonuniform moving sampling scheme based on a moving platform," *IEEE Signal Process. Lett.*, vol. 28, pp. 1714–1718, 2021.
- [43] C.-L. Liu and P. P. Vaidyanathan, "Remarks on the spatial smoothing step in coarray MUSIC," *IEEE Signal Process. Lett.*, vol. 22, no. 9, pp. 1438–1442, Sep. 2015.
- [44] —, "Robustness of coarrays of sparse arrays to sensor failures," in *Proc. IEEE Int. Conf. Acoust., Speech, Signal Process.*, Apr. 2018, pp. 3231–3235.
- [45] B. Friedlander, "Antenna array manifolds for high-resolution direction finding," *IEEE Trans. Signal Process.*, vol. 66, no. 4, pp. 923–932, Feb. 2018.
- [46] K. Pasala and E. Friel, "Mutual coupling effects and their reduction in wideband direction of arrival estimation," *IEEE Trans. Aerosp. Electron. Syst.*, vol. 30, no. 4, pp. 1116–1122, Oct. 1994.
- [47] E. BouDaHer, F. Ahmad, M. G. Amin, and A. Hoorfar, "Mutual coupling effect and compensation in non-uniform arrays for direction-of-arrival estimation," *Digit. Signal Process.*, vol. 61, pp. 3–14, Feb. 2017.
- [48] Z. Ye, J. Dai, X. Xu, and X. Wu, "DOA estimation for uniform linear array with mutual coupling," *IEEE Trans. Aerosp. Electron. Syst.*, vol. 45, no. 1, pp. 280–288, Jan. 2009.
- [49] B. Liao, Z. G. Zhang, and S. C. Chan, "DOA estimation and tracking of ULAs with mutual coupling," *IEEE Trans. Aerosp. Electron. Syst.*, vol. 48, no. 1, pp. 891–905, Jan. 2012.
- [50] B. Friedlander and A. Weiss, "Direction finding in the presence of mutual coupling," *IEEE Trans. Antennas Propagat.*, vol. 39, no. 3, pp. 273–284, Mar. 1991.
- [51] W. Zheng, X. Zhang, J. Li, and J. Shi, "Extensions of co-prime array for improved DOA estimation with hole filling strategy," *IEEE Sensors J.*, vol. 21, no. 5, pp. 6724–6732, Mar. 2021.



Zixiang Yang received the B.S. degree in electronic and information engineering from the University of Electronic Science and Technology of China, Chengdu, China, in 2017. He is currently working toward the Ph.D. degree with the School of Information and Electronics, Beijing Institute of Technology, Beijing, China. His research interests include array signal processing and radar signal processing.



Qing Shen received his B.S. degree in 2009 and Ph.D. degree in 2016, both from the Beijing Institute of Technology, Beijing, China. He then worked as a Postdoctoral Researcher with the Beijing Institute of Technology, where he is currently an Associate Professor. From 2013 to 2015 and from 2018 to 2019, he was a Sponsored Researcher in the Department of Electronic and Electrical Engineering, University of Sheffield, Sheffield, UK. His research interests include sensor array signal processing, statistical signal processing, adaptive signal processing, and their

various applications to acoustics, radar, sonar, and wireless communications. He was the recipient of two Excellent Ph.D. Thesis Awards from both the Chinese Institute of Electronics and the Beijing Institute of Technology in 2016. He was also the recipient of the Second-Class Prize of the National Award for Technological Invention in 2020, the First-Class Prize of the Science and Technology (Technological Invention) Award from the Chinese Institute of Electronics in 2018, the Second-Class Prize of the Ministerial Level Science and Technology Progress Award in 2014, and the Young Scientist Award from the IEEE ICET 2021. He is currently a member of the Digital Signal Processing Technical Committee of the IEEE Circuits and Systems Society. He is the Financial Co-Chair of the IEEE CAMSAP 2023, and served as the Session Co-Chair of several international conferences.



Wei Liu (S'01-M'04-SM'10) received his BSc and LLB. degrees from Peking University, China, in 1996 and 1997, respectively, MPhil from the University of Hong Kong in 2001, and PhD from University of Southampton, UK, in 2003. He then worked as a postdoc first at Southampton and later at Imperial College London. Since September 2005, he has been with the Department of Electronic and Electrical Engineering, University of Sheffield, UK, first as a Lecturer and then a Senior Lecturer. He has published 380+ journal and conference papers,

five book chapters, and two research monographs titled "Wideband Beamforming: Concepts and Techniques" (Wiley, March 2010) and "Low-Cost Smart Antennas" (Wiley, March 2019), respectively. His research interests cover a wide range of topics in signal processing, with a focus on sensor array signal processing and its various applications, such as robotics and autonomous systems, human computer interface, radar, sonar, and wireless communications. He is a member of the Digital Signal Processing Technical Committee of the IEEE Circuits and Systems Society (Chair from May 2022) and the Sensor Array and Multichannel Signal Processing Technical Committee of the IEEE Signal Processing Society (Chair for 2021-2022). He was an Associate Editor for IEEE Trans. on Signal Processing (2015-2019) and IEEE Access (2016-2021), and is currently an editorial board member of the journals Frontiers of Information Technology and Electronic Engineering and Journal of the Franklin Institute.



Yonina C. Eldar (S'98-M'02-SM'07-F'12) received the B.Sc. degree in Physics in 1995 and the B.Sc. degree in Electrical Engineering in 1996 both from Tel-Aviv University (TAU), Tel-Aviv, Israel, and the Ph.D. degree in Electrical Engineering and Computer Science in 2002 from the Massachusetts Institute of Technology (MIT), Cambridge. She is currently a Professor in the Department of Mathematics and Computer Science, Weizmann Institute of Science, Rehovot, Israel. She was previously a Professor in the Department of Electrical Engineering at the Technion. She is also a Visiting Professor at MIT, a Visiting Scientist at the Broad Institute, and an Adjunct Professor at Duke University and was a Visiting Professor at Stanford. She is a member of the Israel Academy of Sciences and Humanities (elected 2017), an IEEE Fellow and a EURASIP Fellow. Her research interests are in the broad areas of statistical signal processing, sampling theory and compressed sensing, learning and optimization methods, and their applications to biology, medical imaging and optics.

Dr. Eldar has received many awards for excellence in research and teaching, including the IEEE Signal Processing Society Technical Achievement Award (2013), the IEEE/AESS Fred Nathanson Memorial Radar Award (2014), and the IEEE Kiyoo Tomiyasu Award (2016). She was a Horev Fellow of the Leaders in Science and Technology program at the Technion and an Alon Fellow. She received the Michael Bruno Memorial Award from the Rothschild Foundation, the Weizmann Prize for Exact Sciences, the Wolf Foundation Krill Prize for Excellence in Scientific Research, the Henry Taub Prize for Excellence in Research (twice), the Hershel Rich Innovation Award (three times), the Award for Women with Distinguished Contributions, the Andre and Bella Meyer Lectureship, the Career Development Chair at the Technion, the Muriel & David Jacknow Award for Excellence in Teaching, and the Technion's Award for Excellence in Teaching (two times). She received several best paper awards and best demo awards together with her research students and colleagues including the SIAM outstanding Paper Prize, the UFFC Outstanding Paper Award, the Signal Processing Society Best Paper Award and the IET Circuits, Devices and Systems Premium Award, was selected as one of the 50 most influential women in Israel and in Asia, and is a highly cited researcher.

She was a member of the Young Israel Academy of Science and Humanities and the Israel Committee for Higher Education. She is the Editor in Chief of Foundations and Trends in Signal Processing, a member of the IEEE Sensor Array and Multichannel Technical Committee and serves on several other IEEE committees. In the past, she was a Signal Processing Society Distinguished Lecturer, member of the IEEE Signal Processing Theory and Methods and Bio Imaging Signal Processing technical committees, and served as an associate editor for the IEEE Transactions On Signal Processing, the EURASIP Journal of Signal Processing, the SIAM Journal on Matrix Analysis and Applications, and the SIAM Journal on Imaging Sciences. She was Co-Chair and Technical Co-Chair of several international conferences and workshops. She is author of the book "Sampling Theory: Beyond Bandlimited Systems" and co-author of five other books published by Cambridge University Press.



Wei Cui received the B.S. degree in physics and Ph.D. degree in Electronics Engineering from Beijing Institute of Technology, Beijing, China, in 1998 and 2003, respectively. From March 2003 to March 2005, he worked as a Post-Doctor in the School of Electronic and Information Engineering, Beijing Jiaotong University. Since then, he has been with the Beijing Institute of Technology, where he is currently a Professor with the School of Information and Electronics. His research interests include adaptive signal processing, array signal processing,

sparse signal processing, and their various applications such as Radar, aerospace telemetry tracking and command. He has published more than 100 papers, holds 52 patents, and received the Ministerial Level Technology Advancement Award twice.